# Using satellite observations to identify and address uncertainties in sources of reactive nitrogen

Eloise Marais (UCL) with Martin Van Damme, Lieven Clarisse, Christine Wiedinmyer, Killian Murphy, Guido van der Werf, Nana Wei, Gongda Lu, Mogesh Naidoo, Rebecca Garland, Keita Sekou

BIRA Seminar   **23 October 2025**
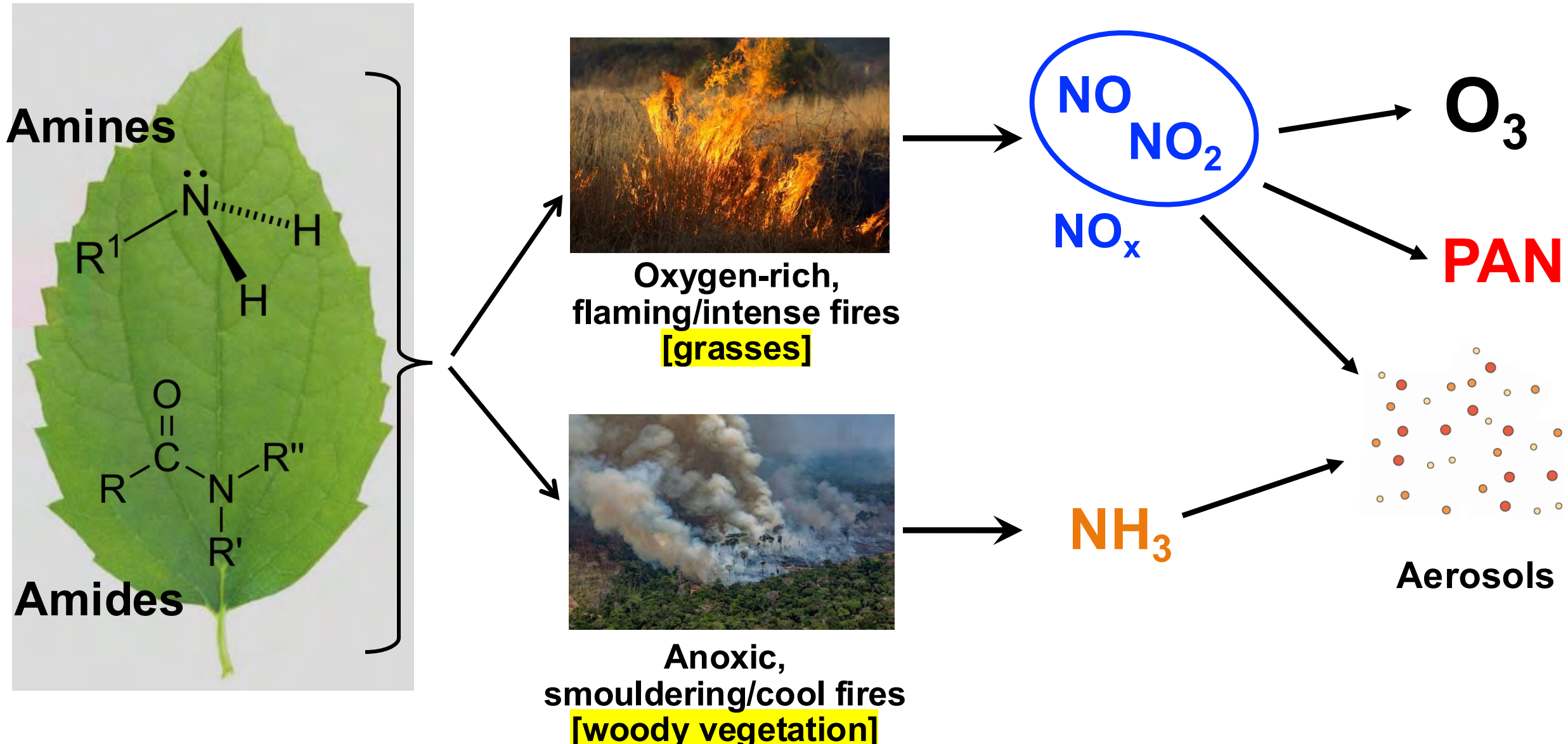
Global Context for Southern Africa Biomass Burning

Biomass burning carbon emissions from the Global Fire Emissions Database (GFED) inventory

650 Tg C (2023)

~10 Tg C (2025)

1100 Tg C (1997)

200 Tg C (2019/2020)

670 Tg C (1997-2016)

[g C m^{-2} yr^{-1}]

[van der Werf et al., 2017]

Open fire emissions in southern Africa outcompete most anomalous fires in other regions, so is a potentially large global source of reactive nitrogen
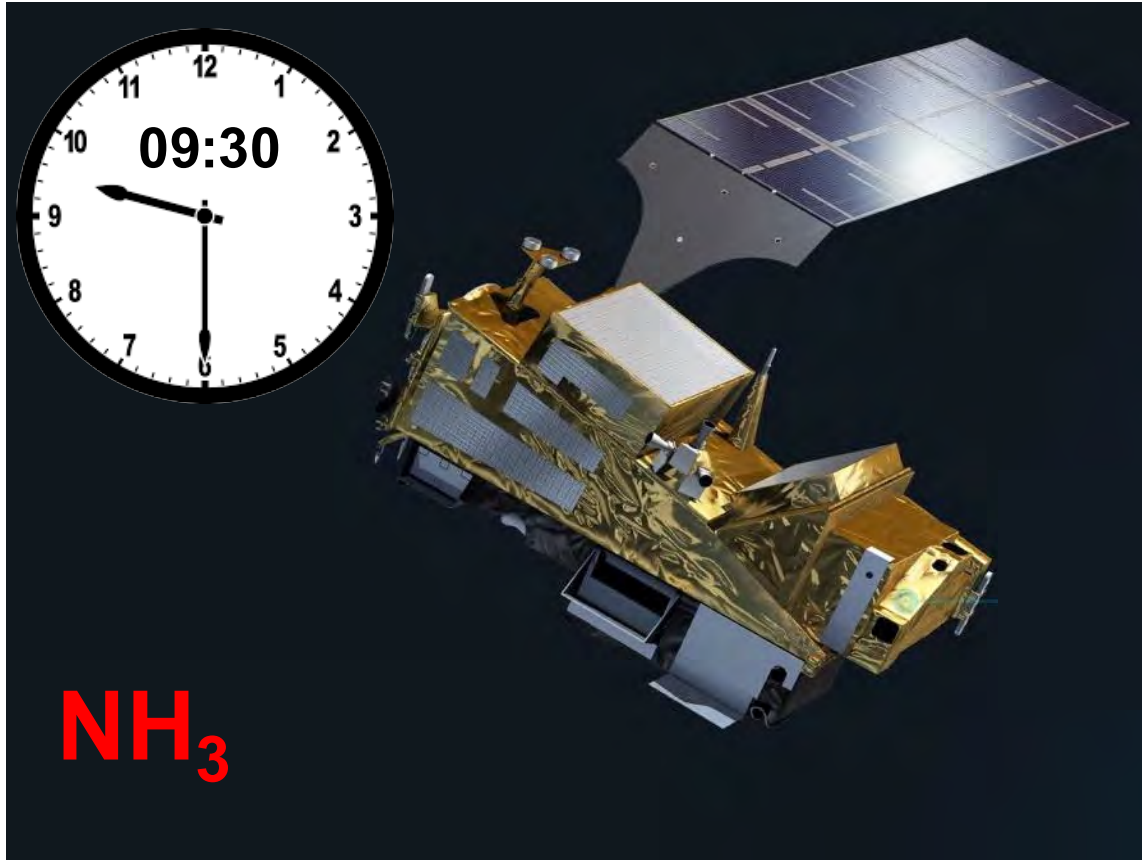
Open Fire Emissions of Reactive Nitrogen

Amines

Amides

Oxygen-rich,
flaming/intense fires
[grasses]

Anoxic,
smouldering/cool fires
[woody vegetation]

NO NO_2
NO_x

O_3

PAN

NH_3

Aerosols

NO_x and NH_3 affect local air quality, regional climate, and global atmospheric composition

Instruments in space measuring NH_3 and NO_2 column densities

IASI: Infrared Atmospheric Sounding Interferometer

TROPOMI: TROPOspheric Monitoring Instrument

09:30

NH_3

13:30

NO_2

Resolution: 12 km (elliptical pixels) at nadir

Swath width: 2200 km

Launch date: 2012

Year used: 2019

Resolution: 5.5 km x 3.5 km at nadir
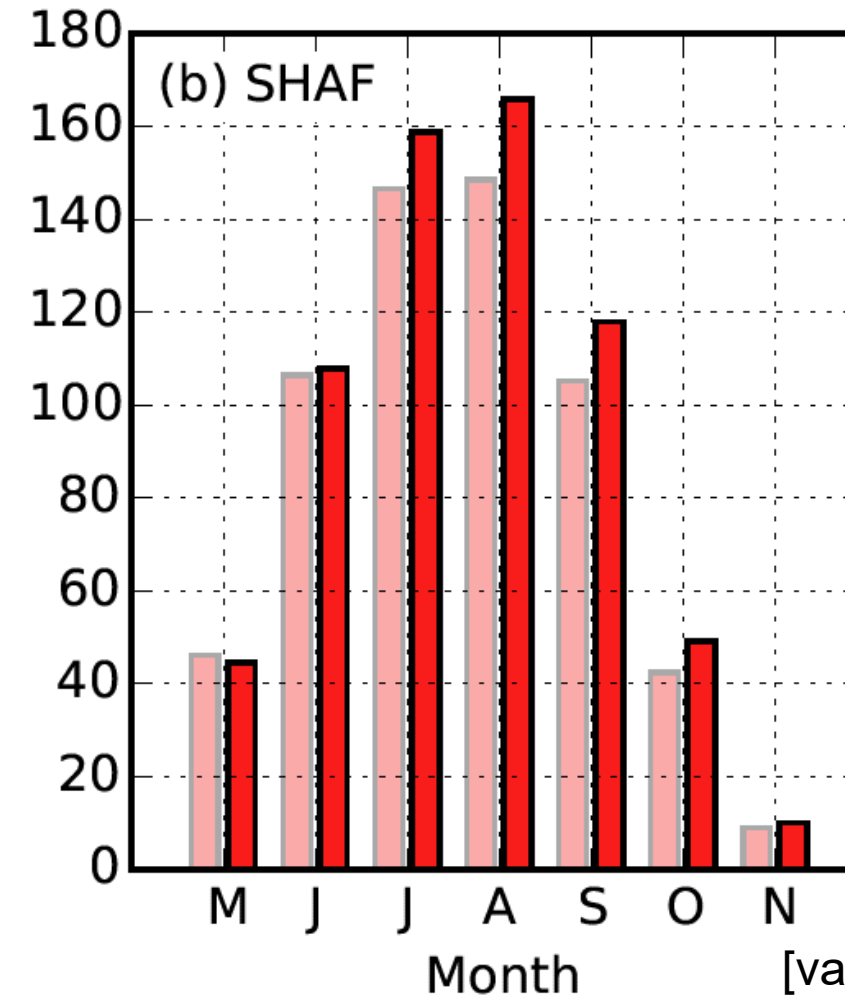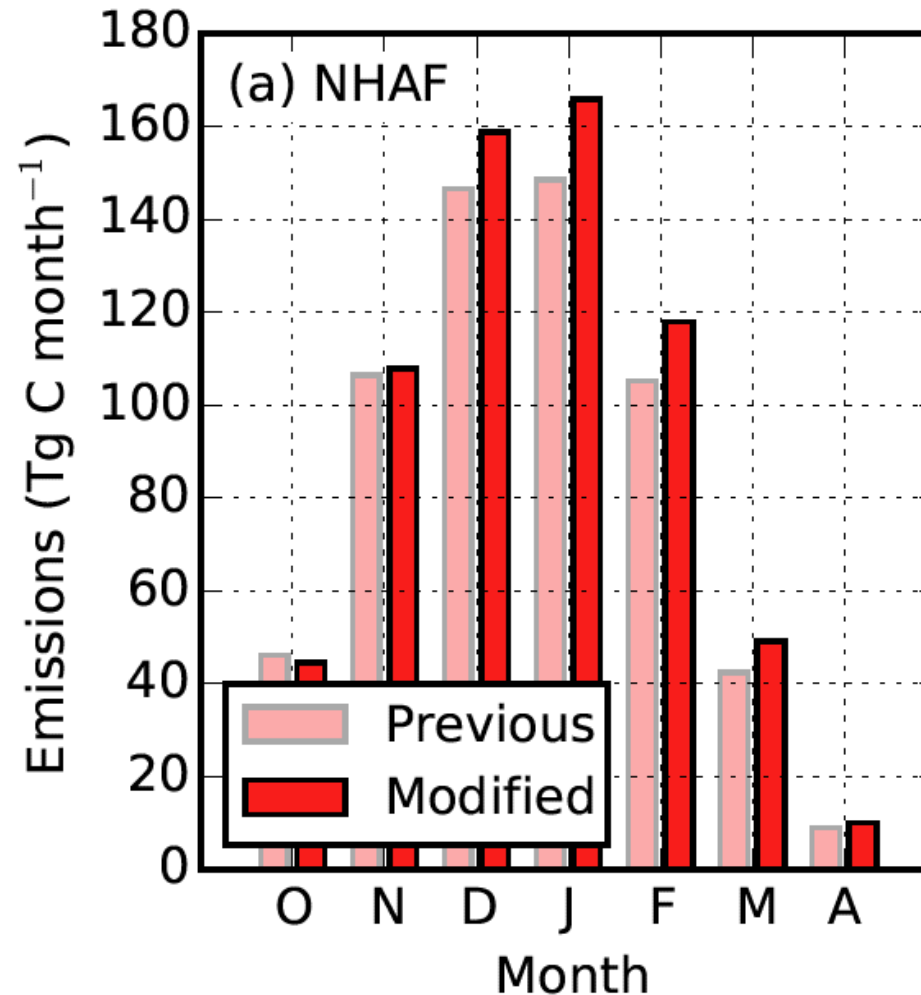
Swath width: 2600 km

Launch date: 2017

Year used: 2019

Seasonality in Southern Africa Biomass Burning

Multiyear mean monthly carbon emissions from biomass burning [Tg C]
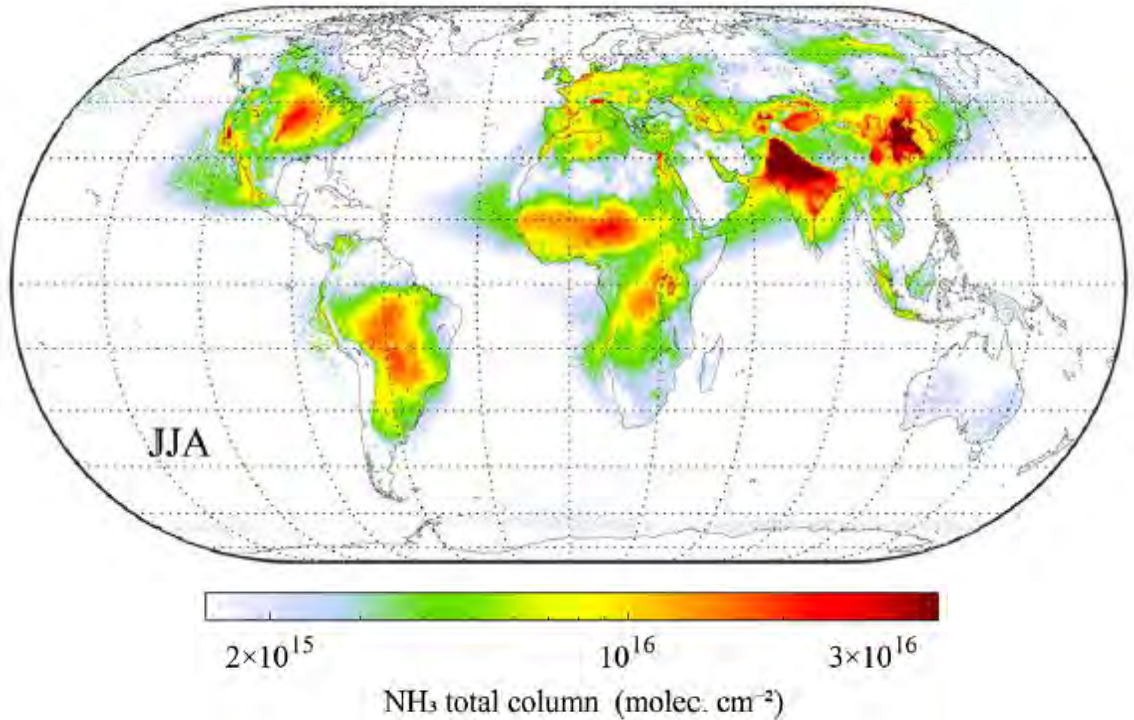
NHAF: NH Africa
SHAF: SH Africa

[van der Werf et al., 2017]

Southern Africa fire season persists for all 6 months of the dry season, peaking in July and August
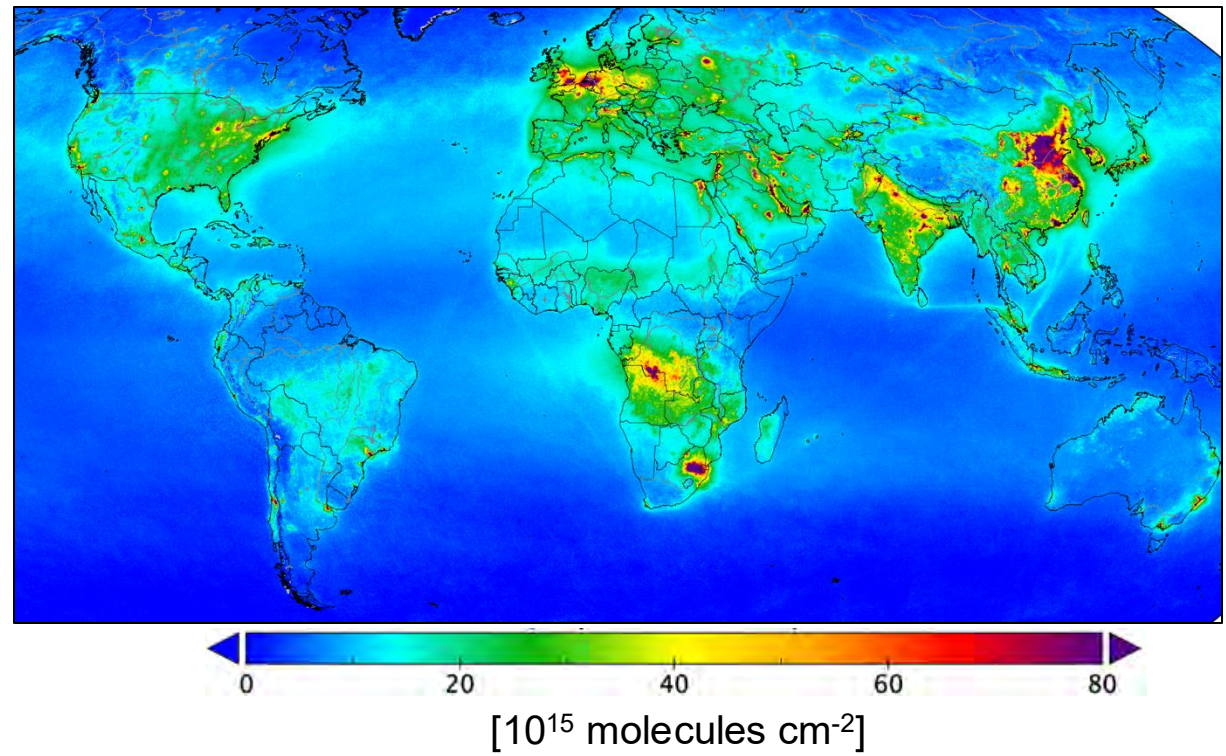
Fires Detected with Both Instruments

IASI multiyear seasonal mean NH_3

TROPOMI annual mean NO_2 (2018-2020)

NH_3 total column (molec. cm^{-2})

[10^{15} molecules cm^{-2}]

[Clarisse et al., 2023]

[https://www.esa.int/Applications/Observing_the_Earth/Copernicus/Sentinel-5P/Nitrogen_dioxide_pollution_mapped]

Instruments provide constraints on NH_3 for IASI and NO_x for TROPOMI NO_2

NO_x and NH_3 account for most reactive nitrogen from open fires

Bottom-Up Biomass Burning Emissions

Emission = DMB x EF

DMB: dry matter burned

EF: emission factor

DMB = Area burned x above-ground biomass x combustion completeness

3 prominent inventories:
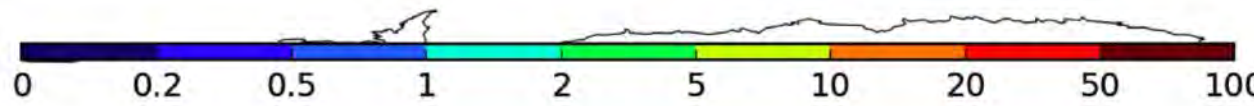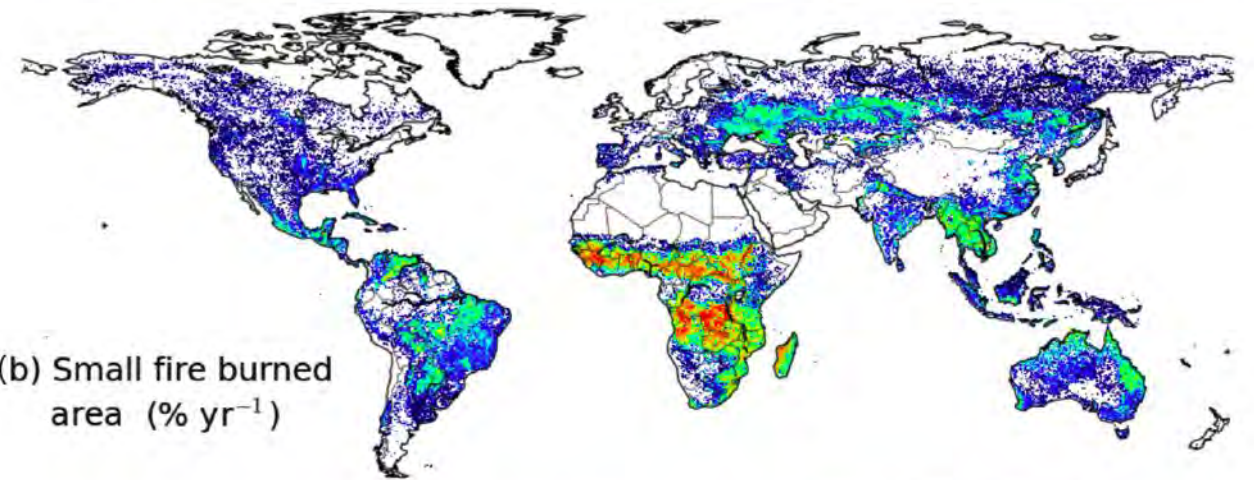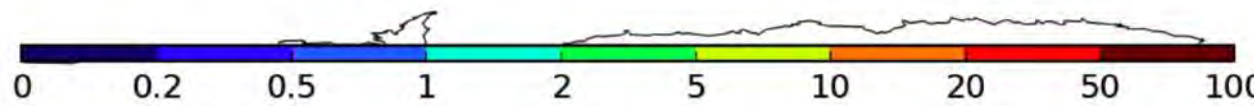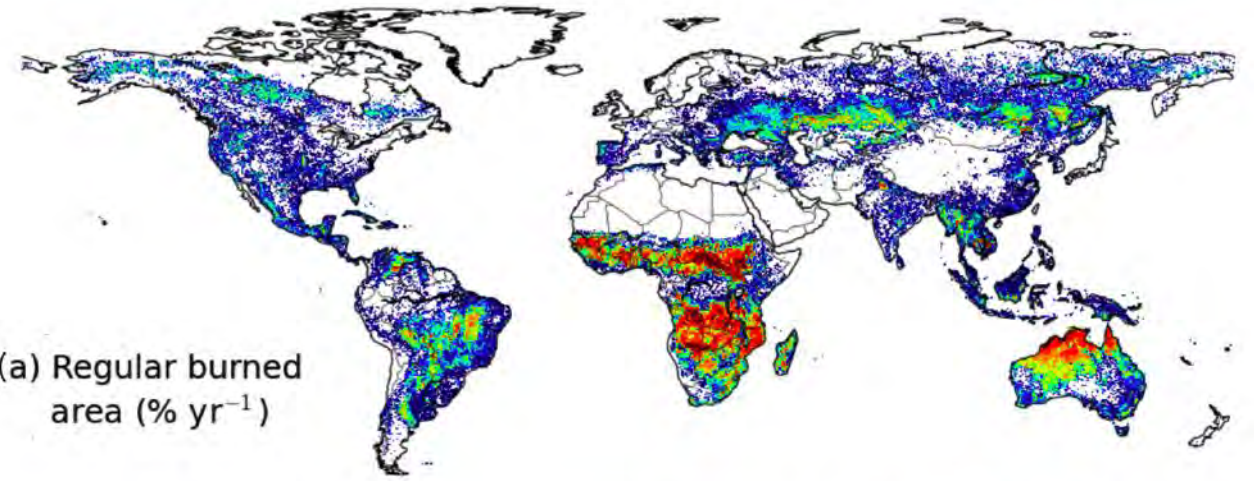
    GFED: Global Fire Emissions Database

    FINN: FIre INventory for NCAR

    GFAS: Global Fire Assimilation System (CAMS)

DMB determined using distinct satellite data products for each inventory

GFED Uses Burned Area

(a) Regular burned area (% yr^{-1})

(b) Small fire burned area (% yr^{-1})

Small fires:
Parameterization that uses MODIS fire counts
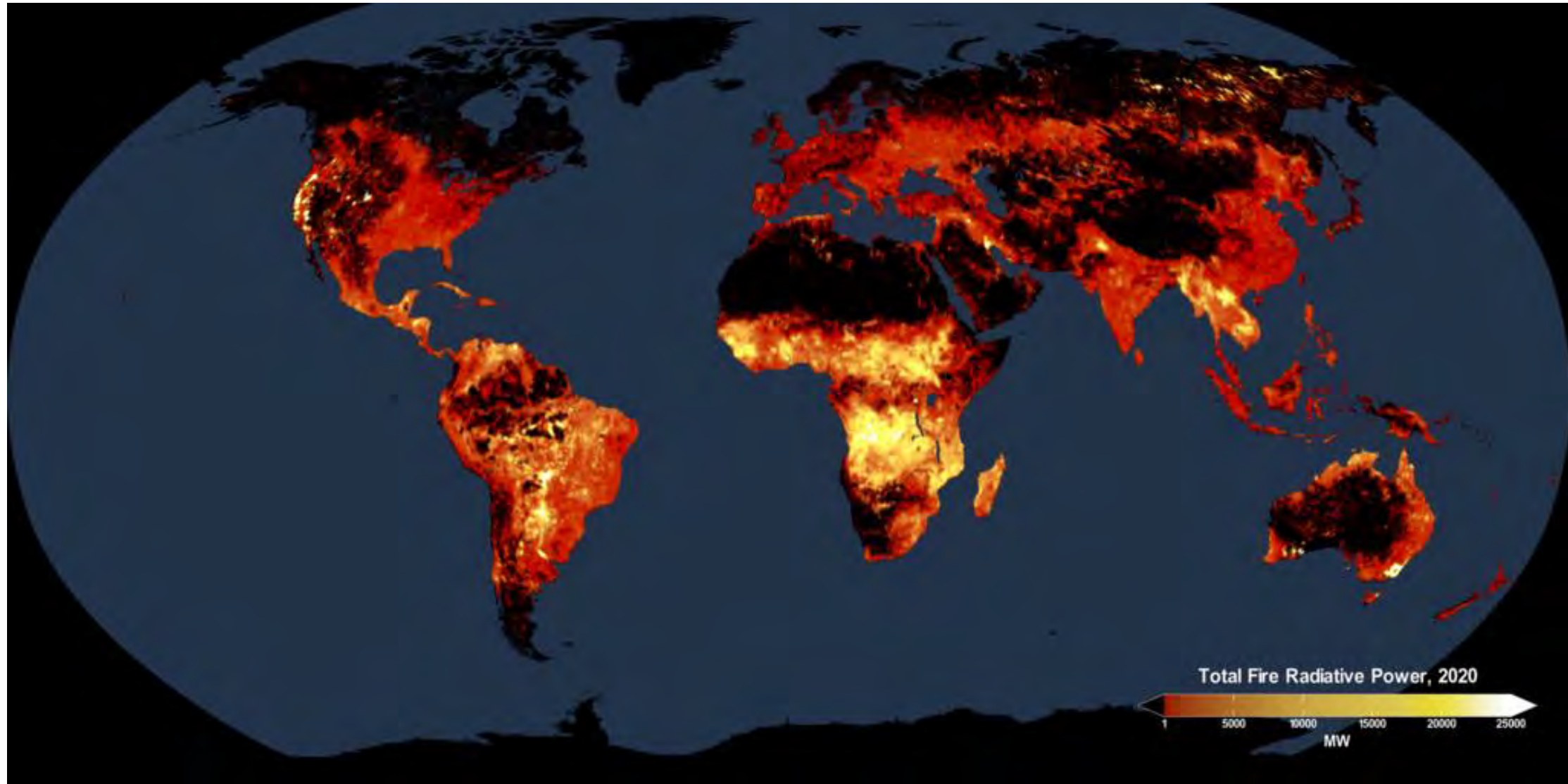
[van der Werf, 2017]

FINN Uses Fire Counts

Jan 20, 2012

Data from MODIS (1 km) and more recent finer resolution VIIRS (375 m)

GFAS Uses Fire Radiative Power

Total Fire Radiative Power, 2020

1   5000   10000   15000   20000   25000
MW

Landcover Specific Emission Factors (EF)

$$Emission = DMB \times \boxed{EF}$$

MODIS Landcover
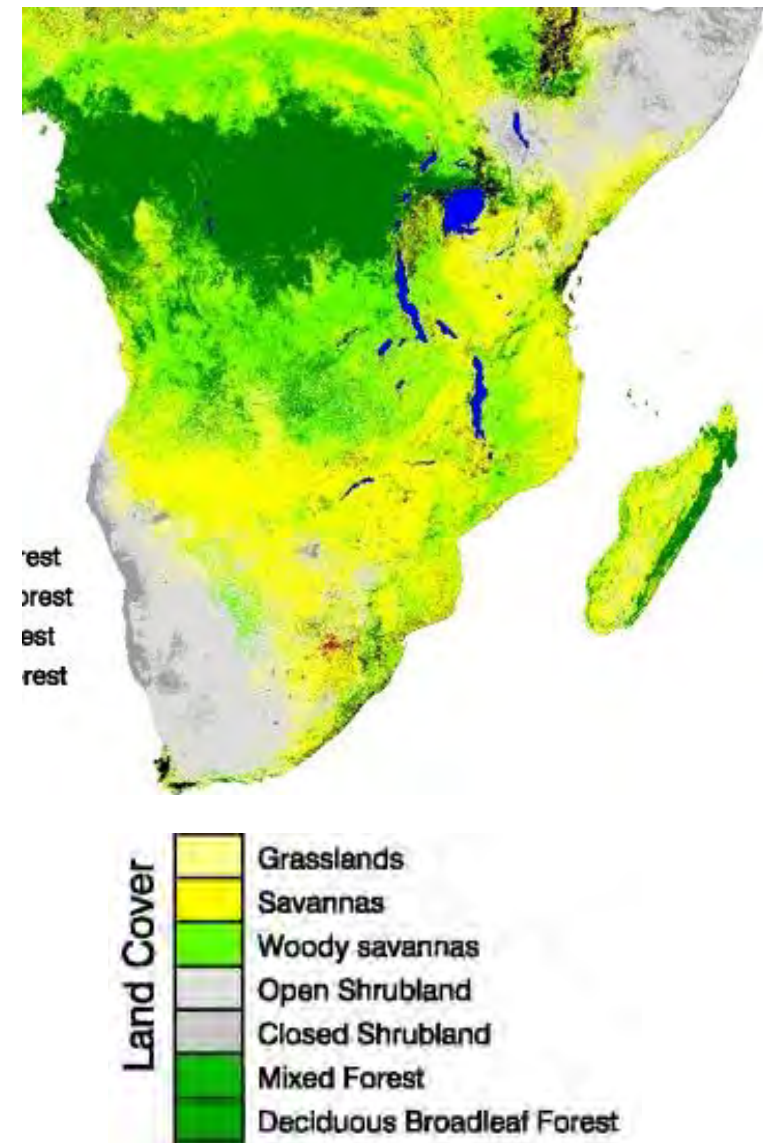
Vegetation type	Emission factor [g kg^{-1}] [a]		
	GFEDv4s	FINNv2.5 [b]	GFASv1.2
NO$_x$ as NO			
Tropical forest	2.55	2.6	2.3
Savanna	3.9	3.9	2.1
Woody savanna [c]	–	3.65	–
NH$_3$			
Tropical forest	1.33	1.3	0.93
Savanna	0.52	0.56	0.74
Woody savanna [c]	–	1.2	–

[Marais et al., 2025]

Biggest difference for NO$_x$ applied to savannas
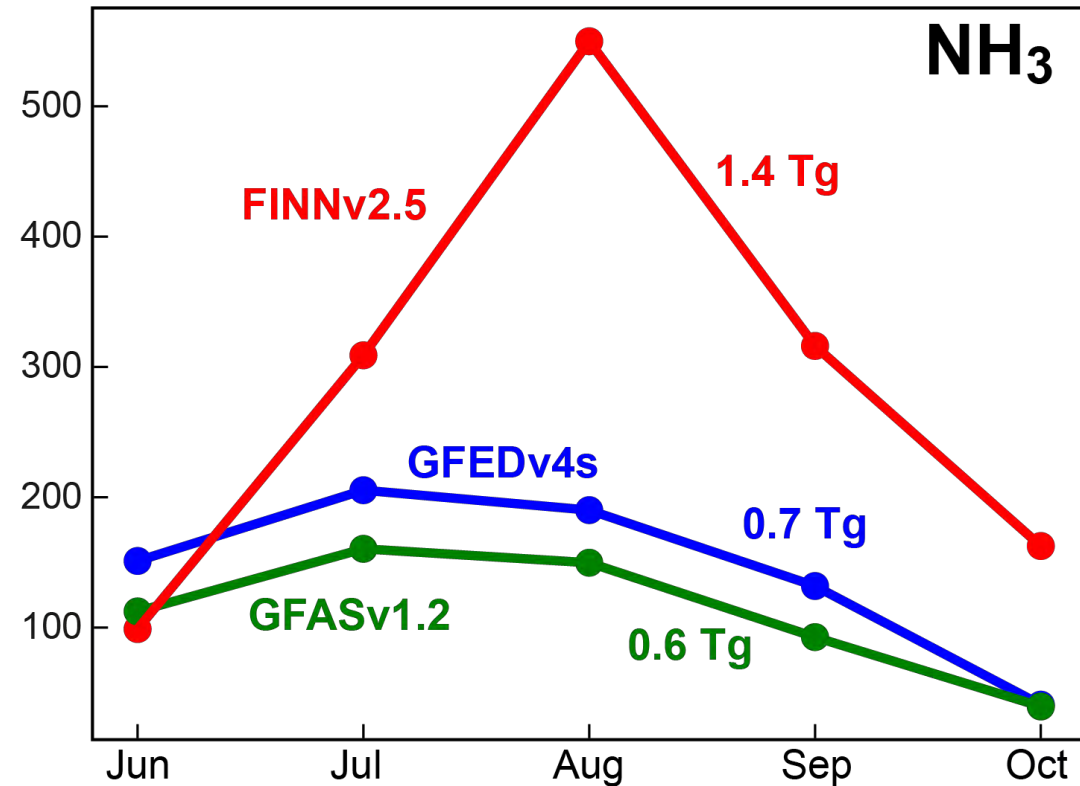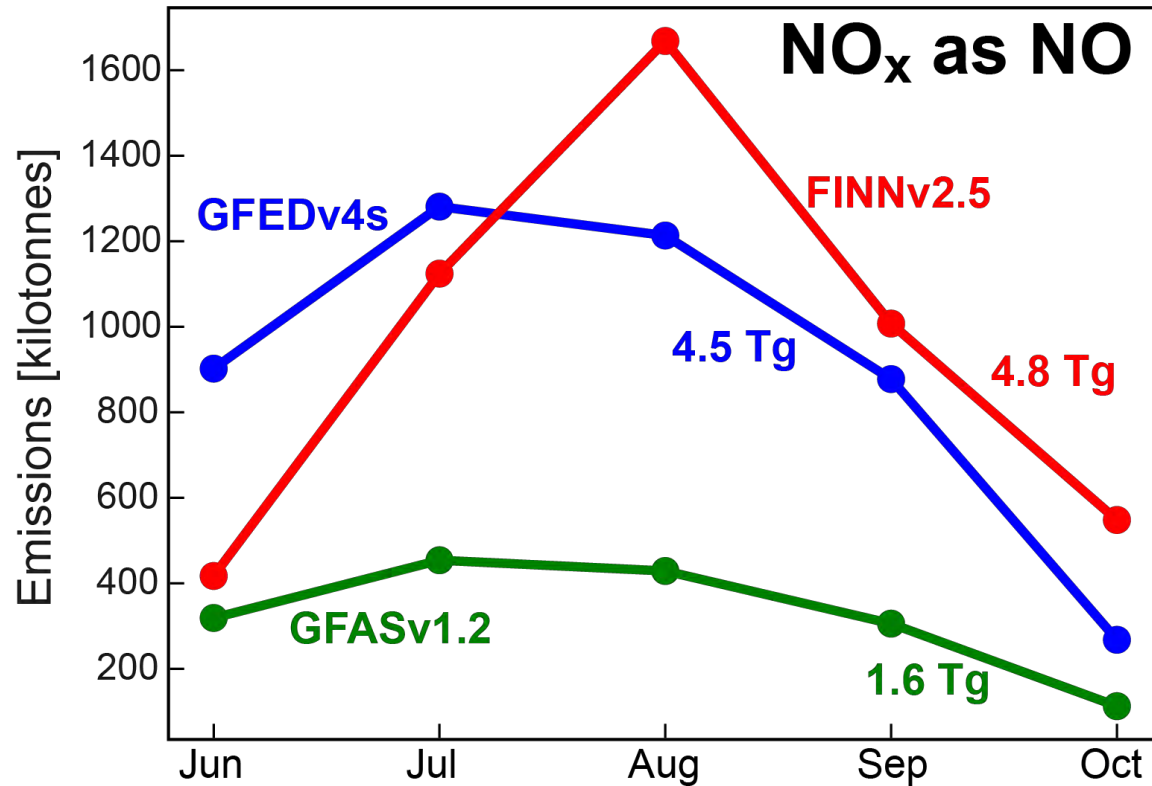
FINN emits NO$_x$ as NO and NO$_2$

Land Cover:
- Grasslands
- Savannas
- Woody savannas
- Open Shrubland
- Closed Shrubland
- Mixed Forest
- Deciduous Broadleaf Forest

Reactive Nitrogen Emissions in Southern Africa

Monthly bottom-up June-October 2019 emissions

Other differences: Time and spatial resolution, injection height, landcover classes

Mostly savanna fires

In FINN, ~20-times more fuel consumed for tropical forest fires (smouldering) than the other inventories

Drive GEOS-Chem with all Three Inventories

GEOS-Chem

Model nested over southern Africa

Emissions

Chemistry, transport, deposition
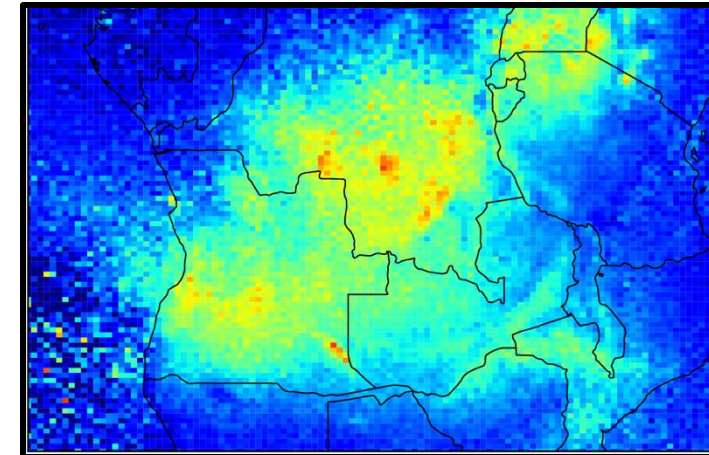
NASA GEOS-FP Meteorology

Driven with 3 difference biomass burning inventories
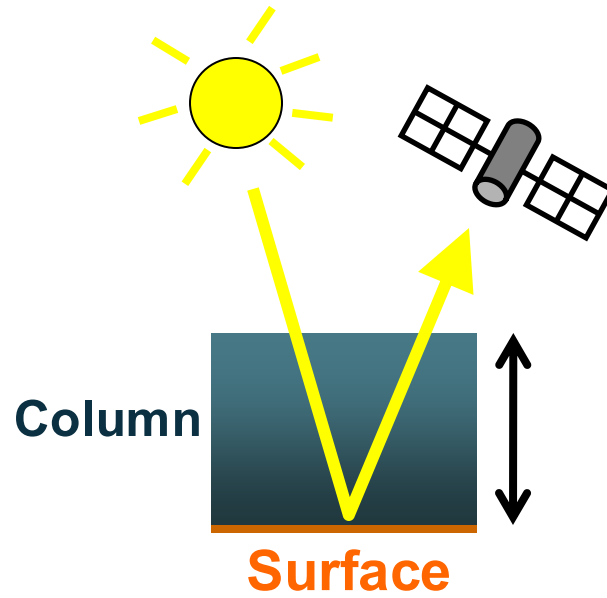
**3D concentrations of NO$_2$, NH$_3$ converted to column densities**

Simulate model with each inventory turned on to compare the model to IASI and TROPOMI
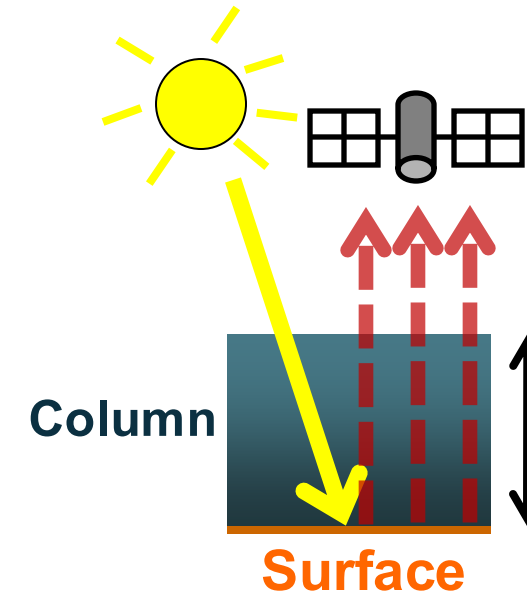
Sample the model at the same overpass time as the instruments

Account for Instrument Vertical Sensitivities

UV-visible instrument (TROPOMI)

Infrared instrument (IASI)

Column

Surface

Column

Surface

Sensitivity peaks in mid troposphere

Different approach for each instrument:
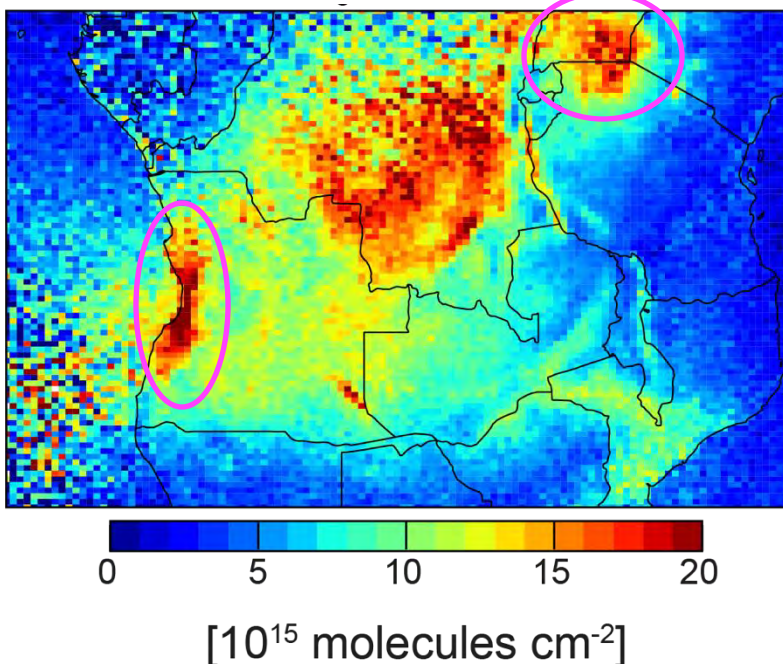
TROPOMI: apply averaging kernels (quantifies vertical sensitivity) to GEOS-Chem

IASI: reprocess (re-retrieve) IASI NH_3 with local GEOS-Chem a priori profiles
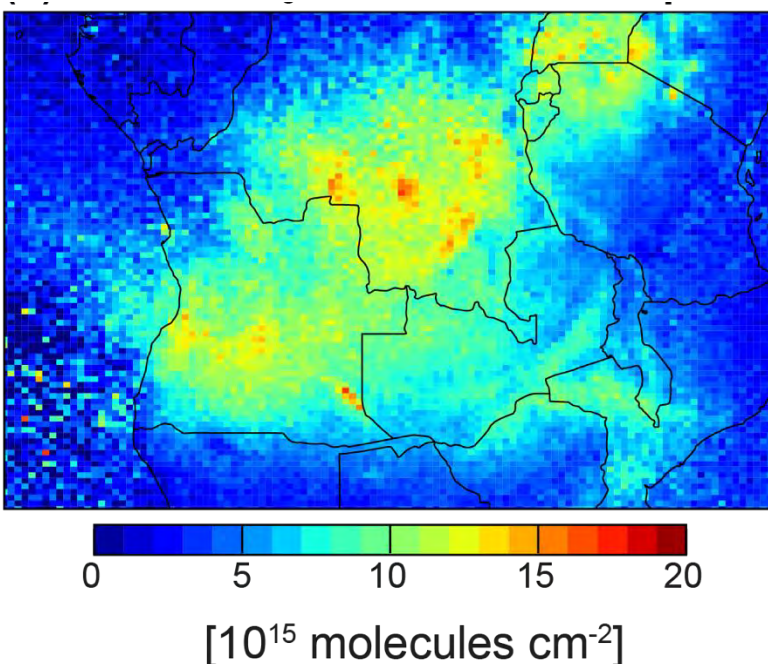
Reprocess IASI with Local GEOS-Chem Priors

IASI columns for July-October 2019. Prior from GEOS-Chem using FINN
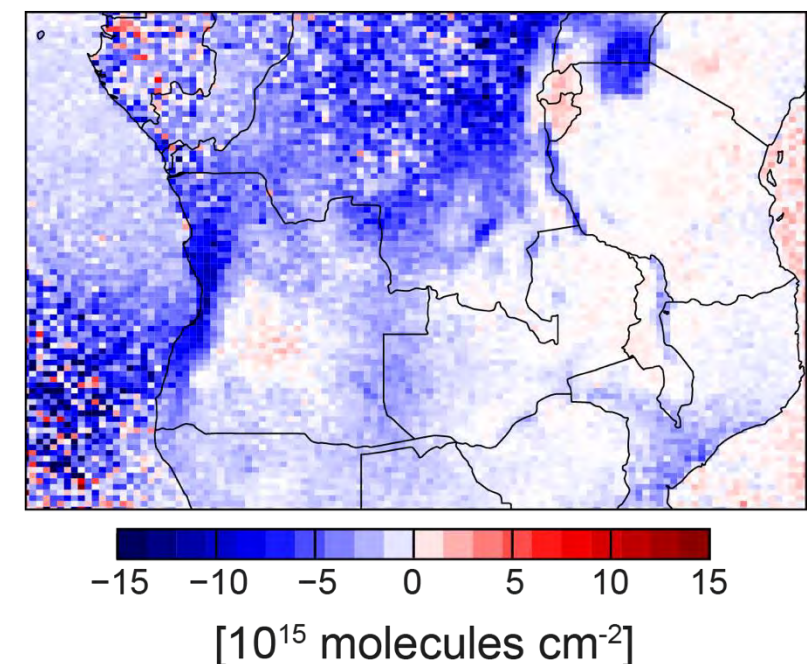
(a) Default prior

(b) GEOS-Chem prior

(b) minus (a)

$[10^{15}$ molecules cm$^{-2}]$

$[10^{15}$ molecules cm$^{-2}]$

$[10^{15}$ molecules cm$^{-2}]$
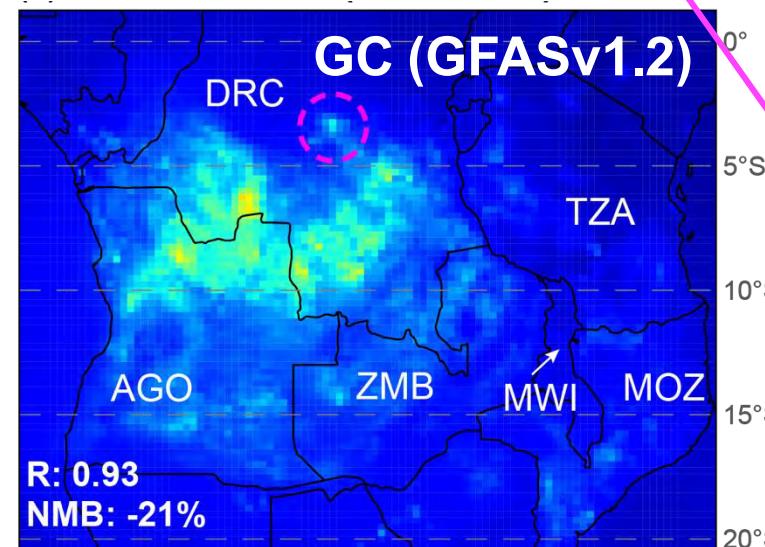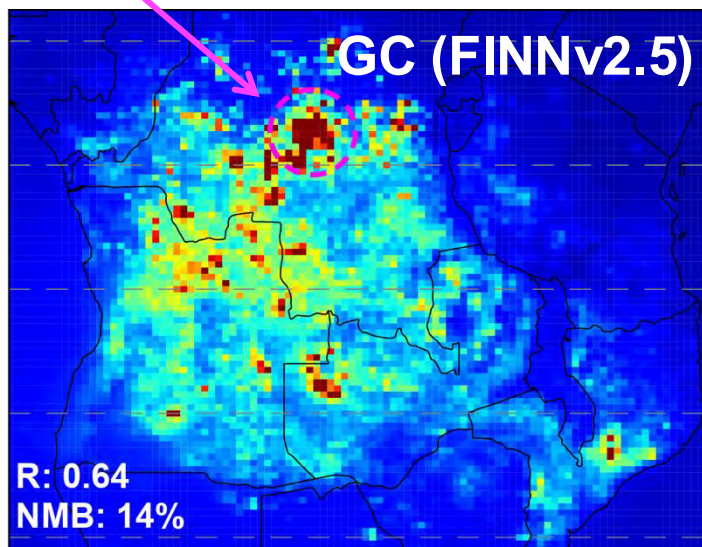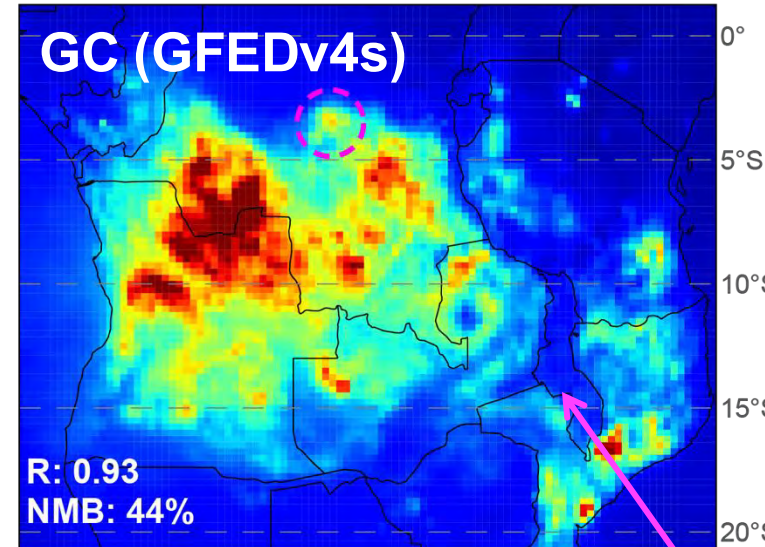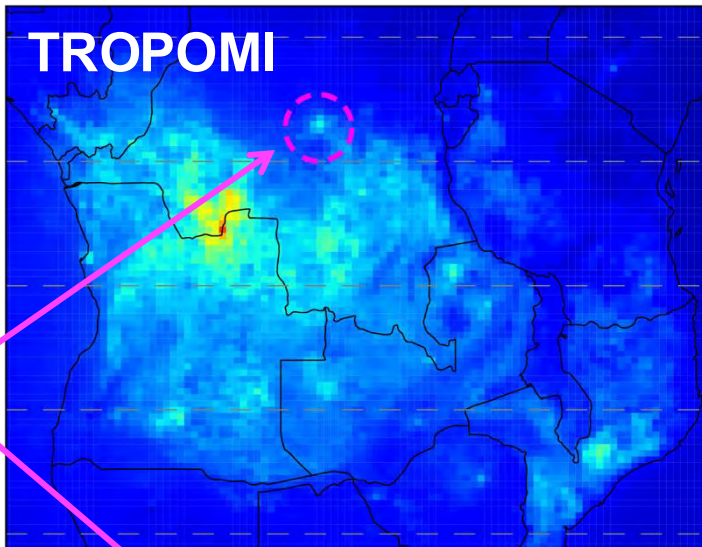
Overall decline in columns with local a priori, as more NH$_3$ placed higher up

Less noisy over Atlantic Ocean east of Angola and northern Namibia

More retrievals pass quality checks

Evaluate Inventory NO$_x$ Emissions with TROPOMI NO$_2$

NO$_2$ vertical column densities for Jun-Oct 2019

GC: GEOS-Chem

Far more NO$_x$ from tropical forests in FINN (fuel load)

GFED and GFAS NO$_2$ spatially similar, but >50% difference due to emission factors

Low emissions in Malawi, as spread of fire suppressed by dense population

Impact of Different NO_x Emissions on Ozone Formation

Ozone production efficiency (**OPE**) = ozone produced per mass unit NO_x emitted

GFAS: **13 Tg O_3 (Tg NO)$^{-1}$**

FINN: **9.6 Tg O_3 (Tg NO)$^{-1}$**

GFED: **6.9 Tg O_3 (Tg NO)$^{-1}$**

FINN OPE > GFED OPE, as far more VOCs and CO in FINN:
    FINN: 108 Tg CO and 13 Tg C for 21 NMVOCs
   **GFED**: 82 Tg CO and 2 Tg C for 13 NMVOCs
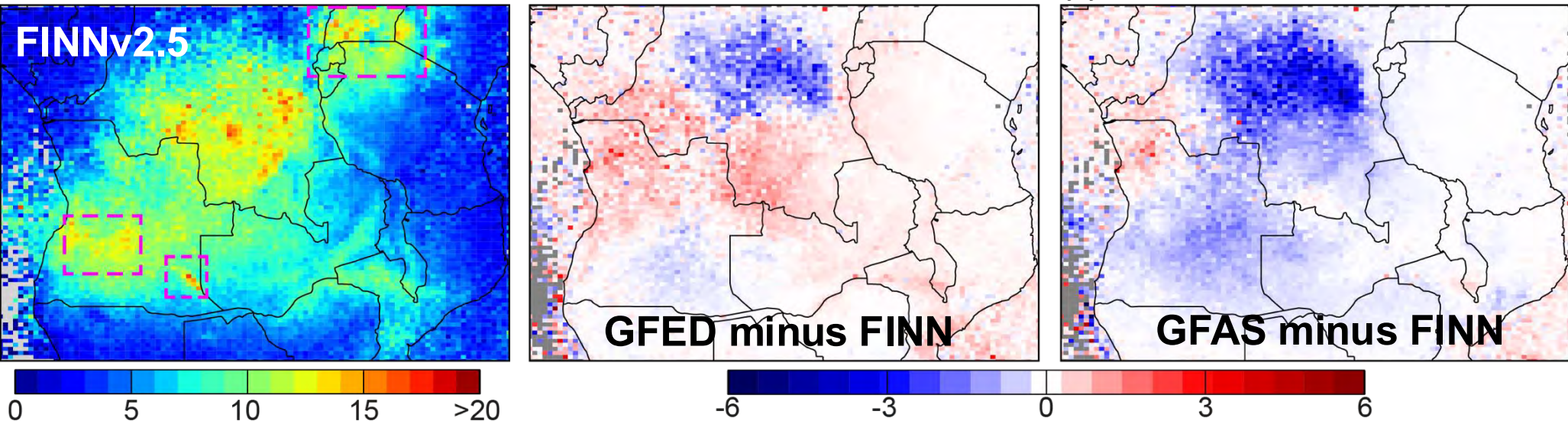
Less NO_x from GFAS increases OPE, as O_3 more sensitive to NO_x
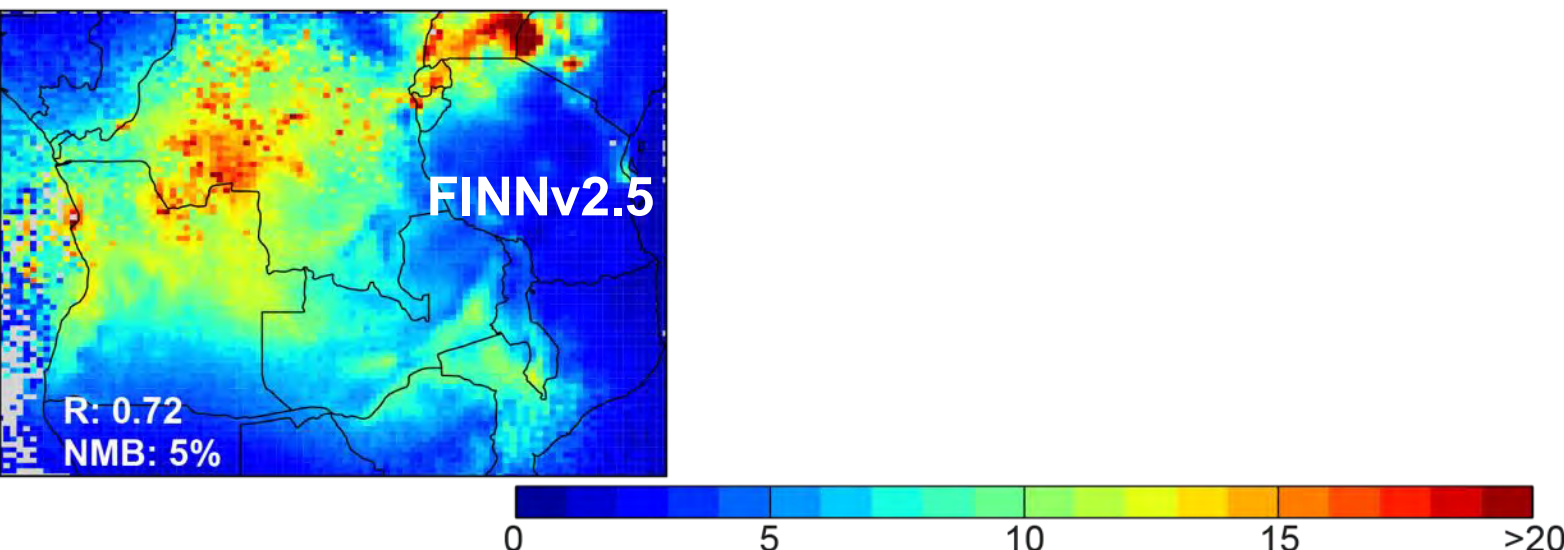
Evaluation of Inventories with Satellite Observations

NH$_3$ vertical column densities for Jul-Oct 2019 [10^{15} molecules cm^{-2}]

IASI with GEOS-Chem prior:

GEOS-Chem:
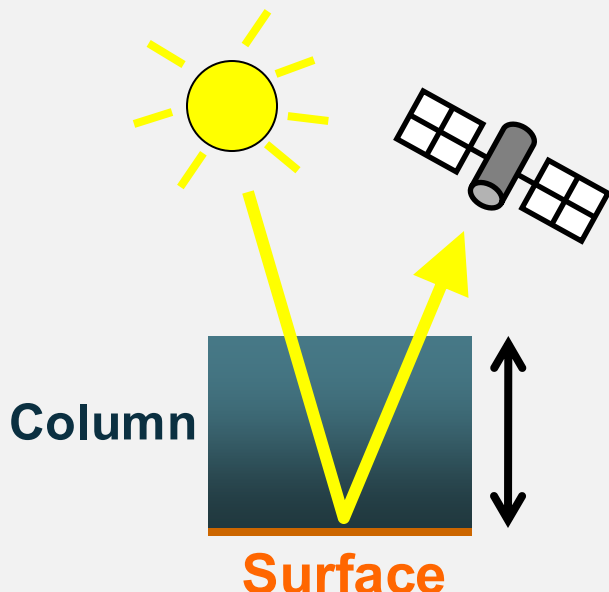
June excluded, as no inventories consistent with IASI observations (R < 0.5)

Top-down emissions estimate
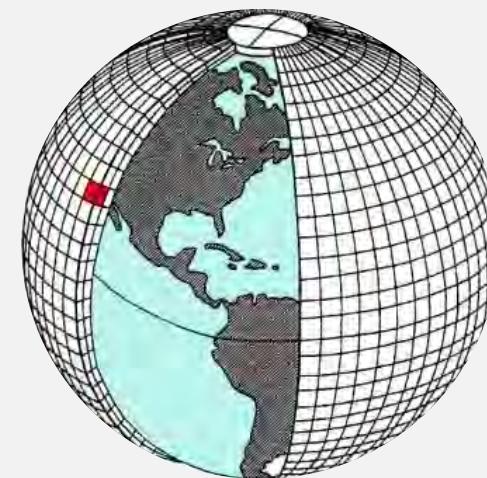
Convert atmospheric **column concentrations** to surface **emissions** using a **model**

COLUMNS	➡	Conversion Factor	➡	EMISSIONS

Satellite columns

**Column-to-Emission ratio (model)**
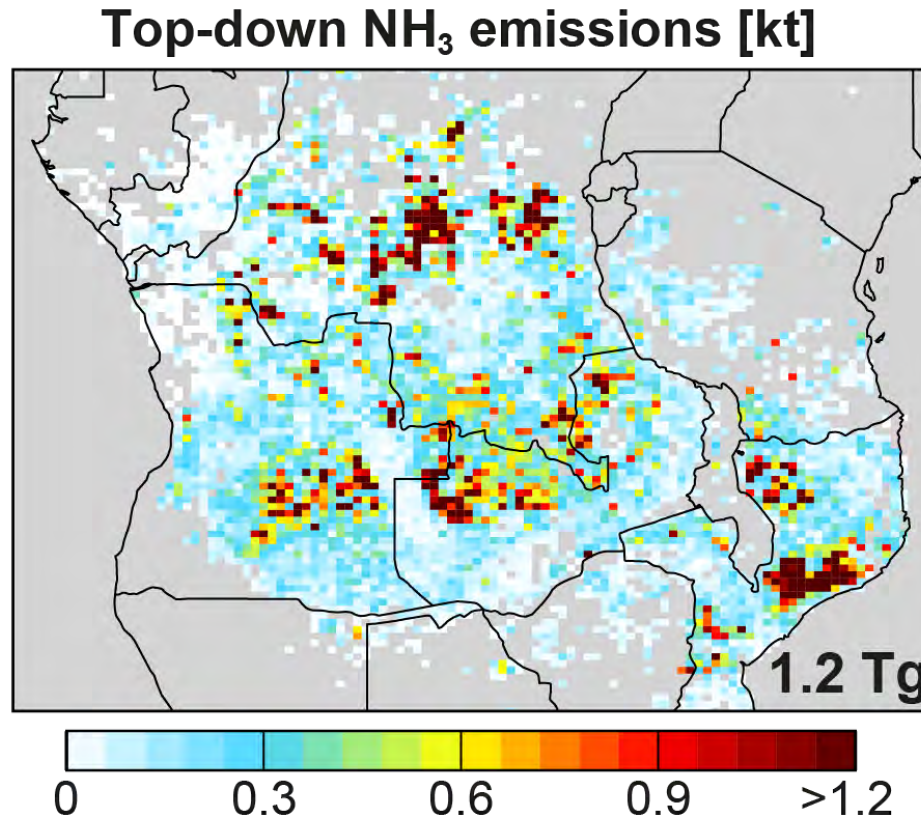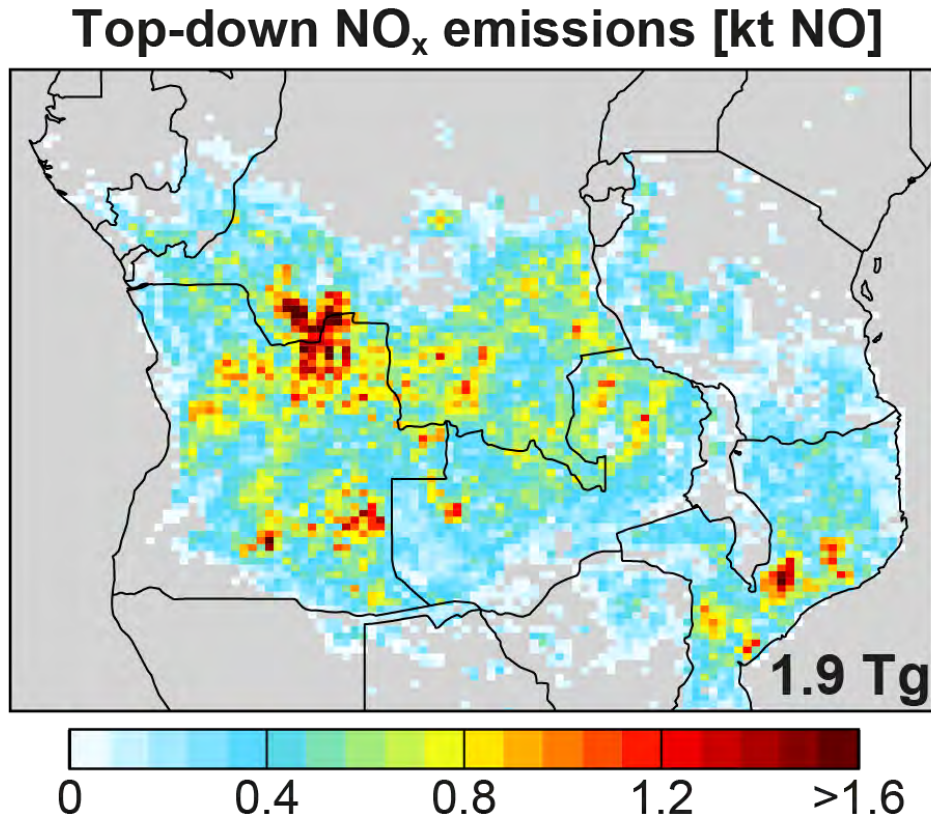
Satellite-derived surface emissions

Emission

Column

Surface

Simple mass balance approach, as it's a first order problem (very large errors)

Use best-performing inventory (**GFAS** for NO_x, **FINN** for NH_3) for gridsquares where open fires > 50% total emissions

Top-down Emissions with Best Performing Inventories

Top-down NO_x emissions [kt NO]

Top-down NH_3 emissions [kt]

Distribution normal for NO_x, long-tailed for NH_3
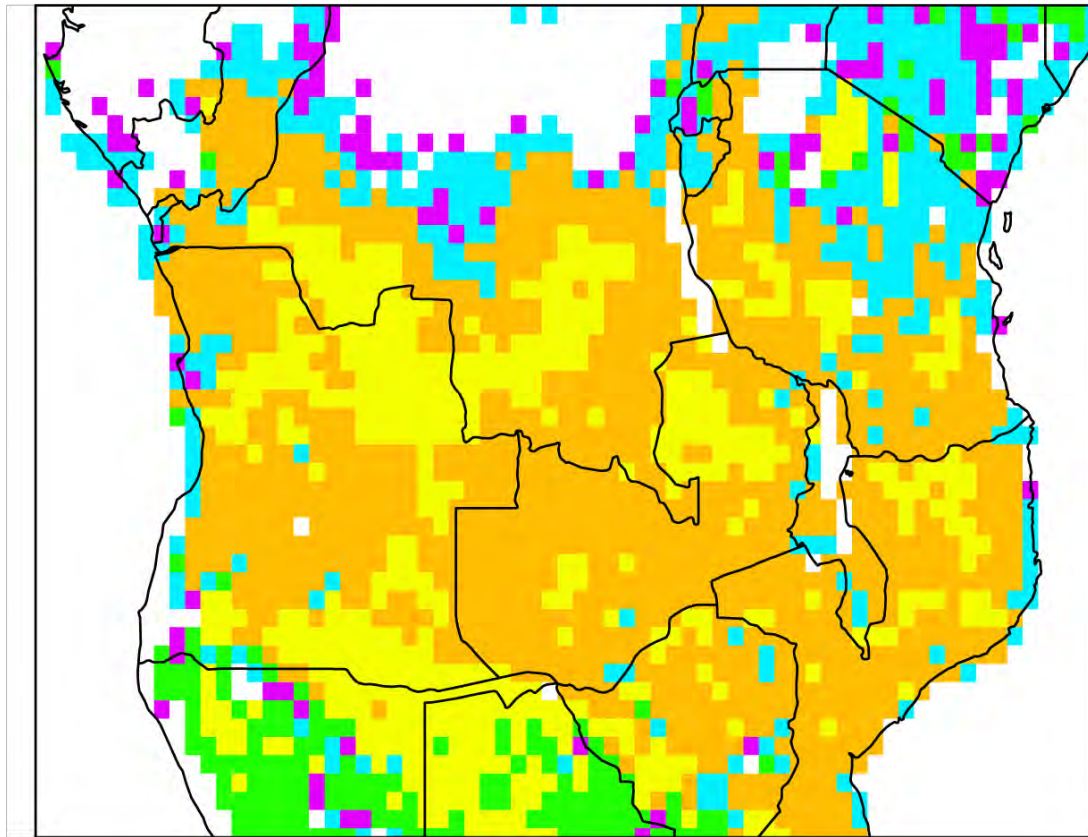
Correlation between top-down NO_x and NH_3 weak (R < 0.4), but strong in inventories (R > 0.8), as none account for the impact of combustion efficiency/pyrome regime on emission factors

Emissions peak in similar month to bottom-up: July and August for NO_x and August in NH_3
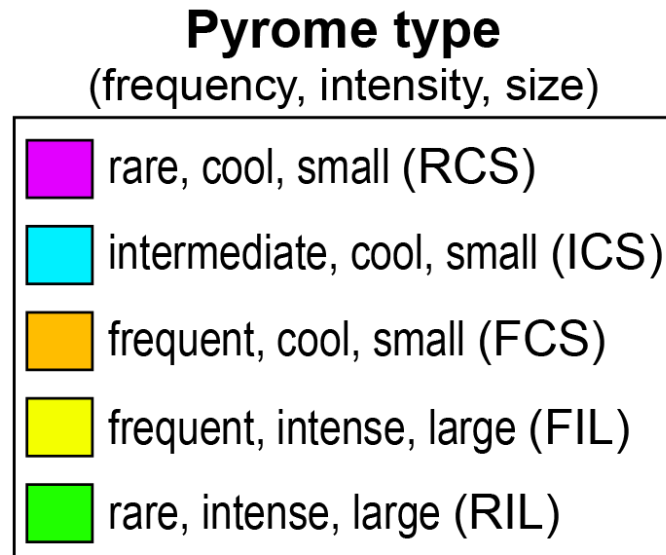
Total anthropogenic emissions in Europe in 2019: ~1.4 Tg N for NO_x and ~8 Tg for NH_3

Consistency of Top-down Emissions and Pyrome Regimes
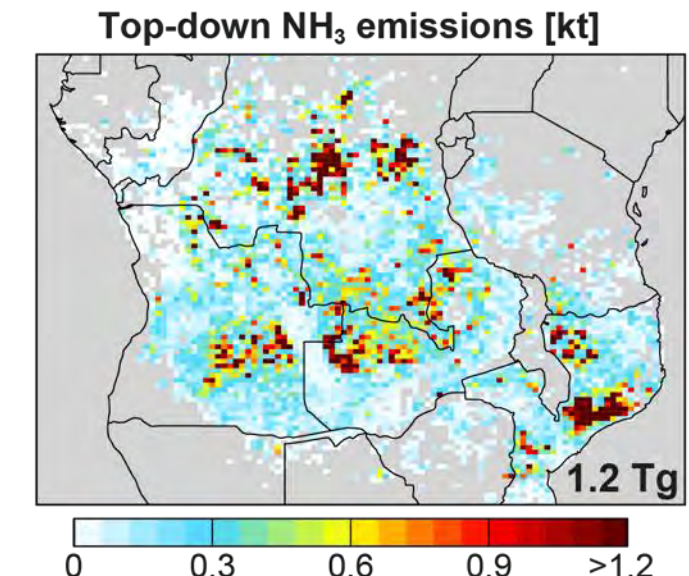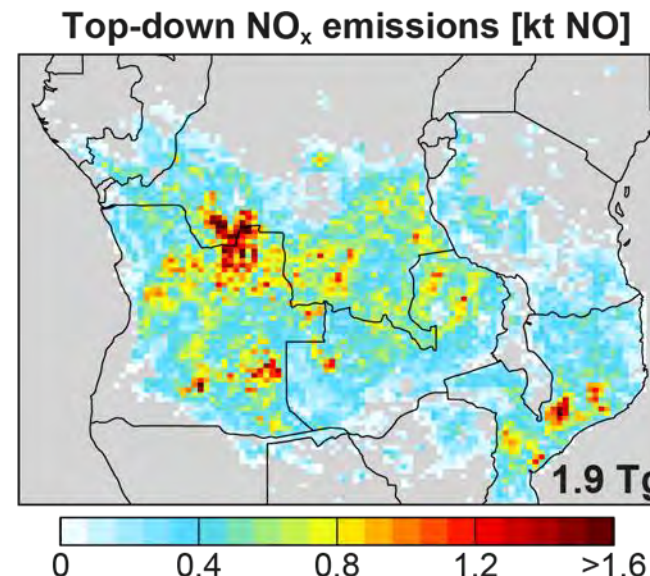
Archibald et al. (2013) pyrome regimes

Pyrome type
(frequency, intensity, size)

- ■ (magenta) rare, cool, small (RCS)
- ■ (cyan) intermediate, cool, small (ICS)
- ■ (orange) frequent, cool, small (FCS)
- ■ (yellow) frequent, intense, large (FIL)
- ■ (green) rare, intense, large (RIL)

NH₃ emissions coincide with cool fires that would tend to smoulder (inefficient)

NO$_x$ emissions coincide with intense fires that would tend to flame (efficient)

Top-down NO$_x$ emissions [kt NO]

1.9 Tg

0   0.4   0.8   1.2   >1.6

Top-down NH₃ emissions [kt]

1.2 Tg

0   0.3   0.6   0.9   >1.2
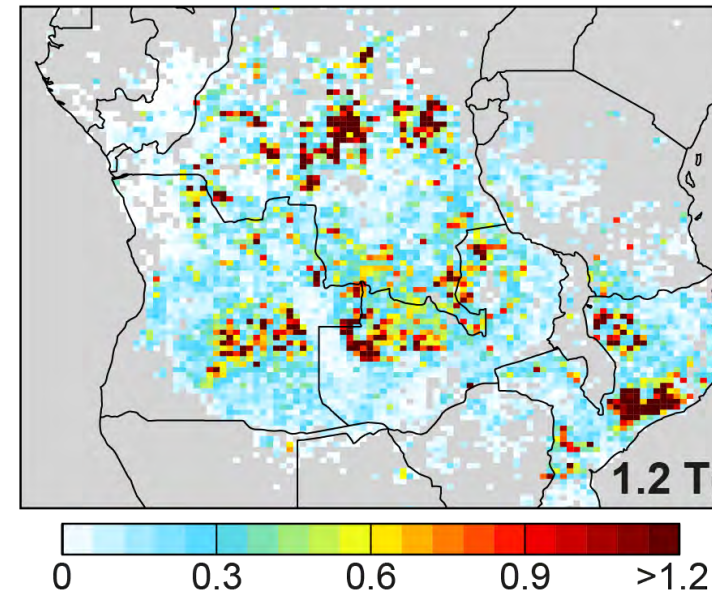
Top-down vs Best Performing Inventory Emissions

Top-down NO$_x$ emissions [kt NO]

Top-down NH$_3$ emissions [kt]

1.9 Tg

1.2 Tg
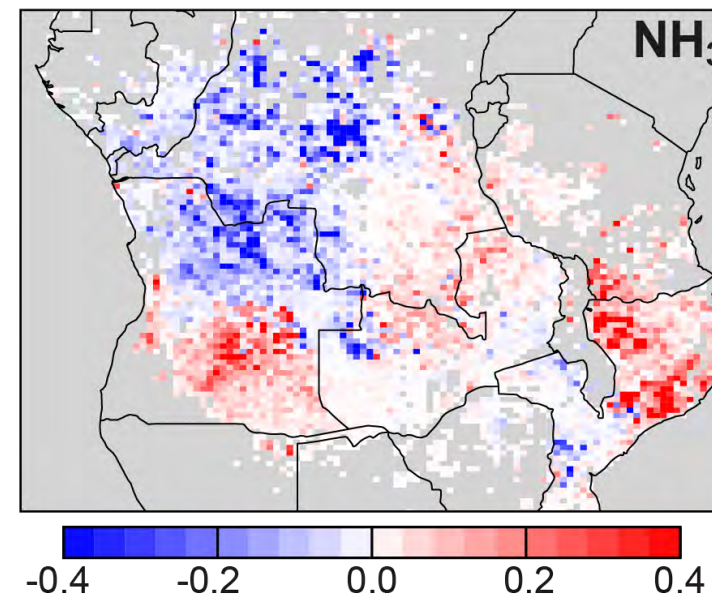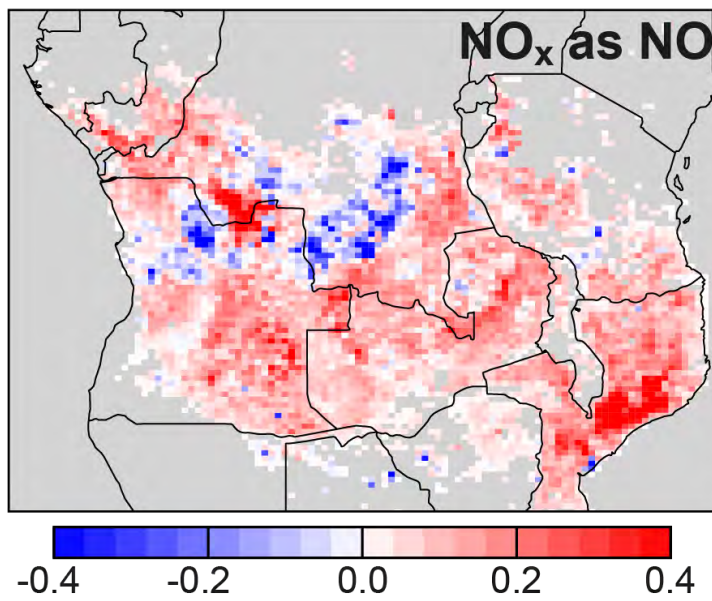
Top-down minus bottom-up emissions [kt]

NO$_x$ as NO

NH$_3$

Observationally constrained ozone production from biomass burning NO$_x$ emissions in southern Africa:

25 Tg O$_3$

Emissions uncertainty estimate (mostly due to instruments):

31% for NO$_x$, 33% for NH$_3$

NO$_x$: 1.9 ± 0.6 Tg NO

NH$_3$: 1.2 ± 0.4 Tg

First Part Summary

Top-down approach could be further refined with more complex inverse modelling methods or with iteration. Regardless, highlights the large disparities between top-down and bottom-up emissions.

Inventories collocate NH_3 and NO_x emissions (smouldering and flaming fires), but these are mostly separate in the top-down estimates

Could adopt hybrid approach: FINN for smouldering fire emissions of NH_3, VOCs, CO, organic aerosols and methane and GFAS or GFED for flaming fire emissions of NO_x, black carbon and CO_2

Choice of emission factors remains an issue without observations to constrain these

Critical need for observations to validate satellite observations and top-down estimates. Ideally in National Parks and in anticipation of geostationary Sentinel-4 IR instrument measuring NH_3 and CO (both markers of smouldering fires)

Invited contribution in Royal Society of Chemistry *Environmental Science: Atmospheres* journal (https://pubs.rsc.org/en/content/articlelanding/2025/ea/d5ea00041f)

Hotspot NO$_x$ Emissions in Sub-Saharan Africa
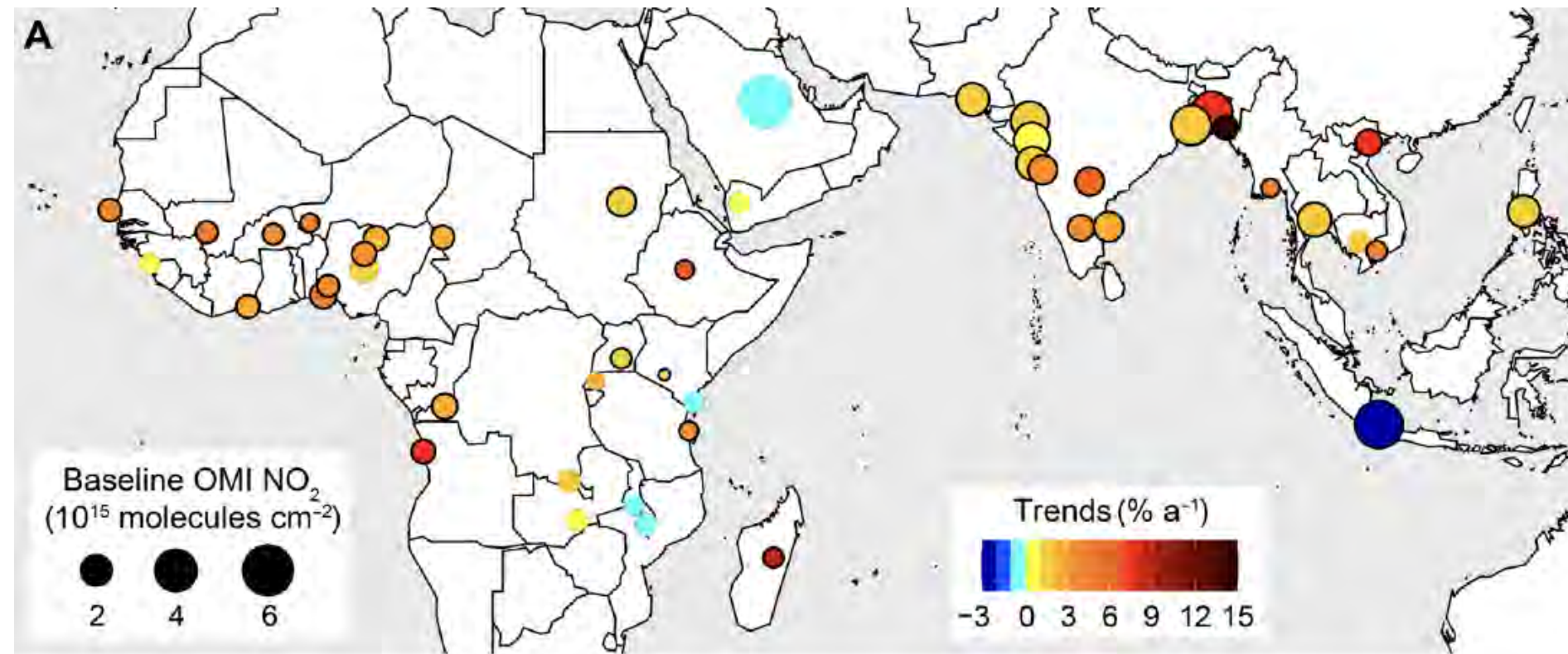
The largest anthropogenic point source emissions of NO$_x$ are in Sub-Saharan Africa (South Africa)

Rank	Lat [° N]	Long [° E]	Emissions [kg s^{-1}]	Error [kg s^{-1}]	Power plants (GPPD)[1]	Cities (WCD)[1]	Comment[2]
1	−26.2875	29.1625	2.76	0.47	Matla; Kriel		
2	−26.5625	29.1625	2.47	0.39			Secunda CTL[3]
3	−23.6875	27.5875	2.47	0.56	Matimba		also Medupi (not listed in GPPD)
4	−26.7375	27.9875	2.03	0.44	Lethabo	Vereeniging	
5	−27.1125	29.7875	2.03	0.31	Majuba		
6	22.3875	82.6875	2.01	0.59	Korba		
7	40.6375	109.7375	1.81	0.57	Baotou	Baotou	
8	21.0125	107.1375	1.80	0.42	Quang Ninh	Ha Long; Cam Pha	
9	−26.0875	28.9875	1.74	0.32	Kendal		
10	−32.4125	151.0125	1.73	0.30	Bayswater; Liddell		

[Beirle et al., 2023]

Unregulated coal-fired power plants (Kriel, Matimba, Lethabo, Majuba, Kendal)
and a synthetic fuels plant (Secunda)

Unprecedented Increases in NO$_x$ in Cities in Africa

2005-2018 trends in Ozone Monitoring Instrument (OMI) NO$_2$ over fast-growing cities in the tropics

A

Baseline OMI NO$_2$
(10^{15} molecules cm^{-2})

2   4   6

Trends (% a^{-1})

-3   0   3   6   9   12   15
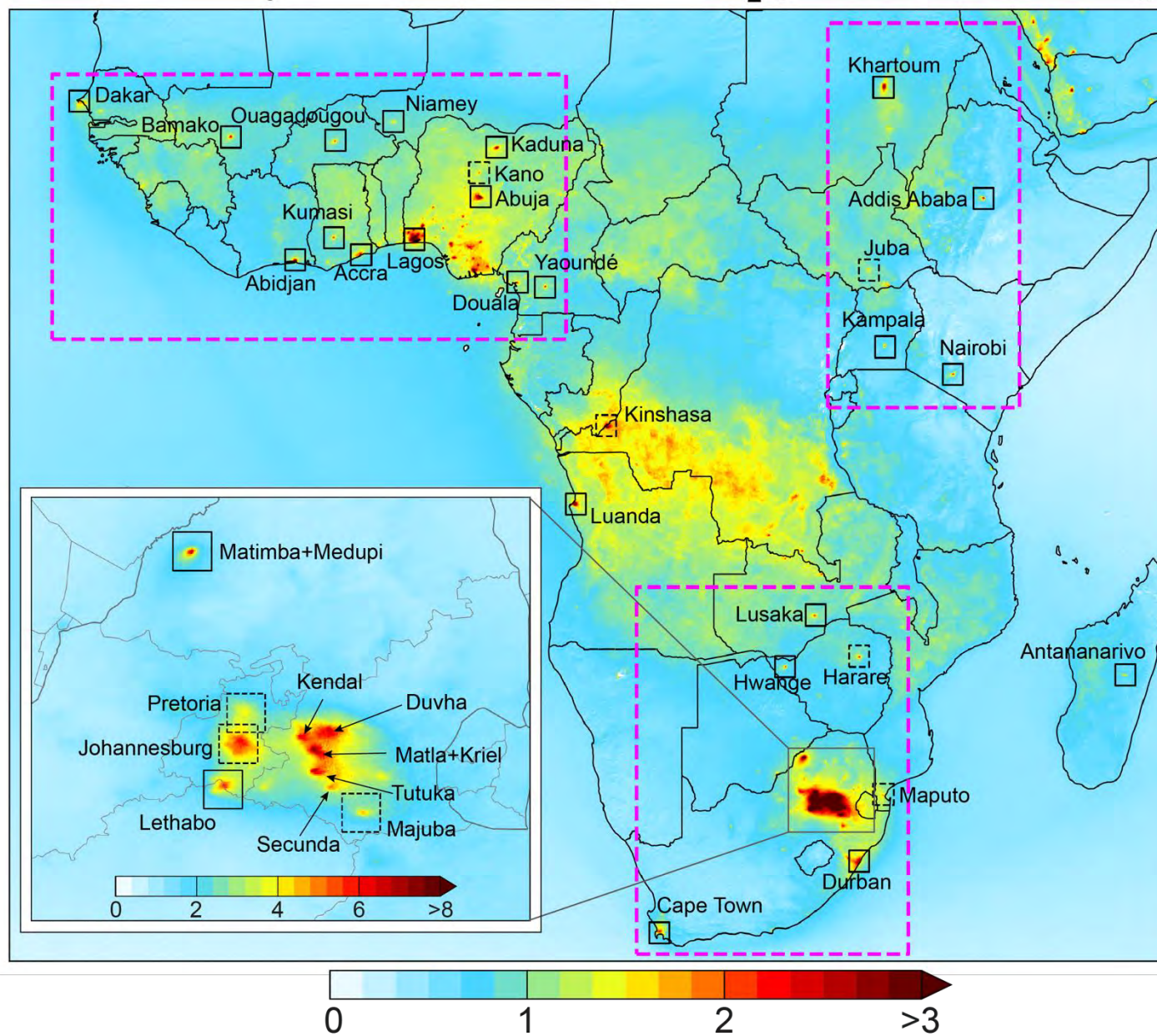
[Vohra et al., 2022]

OMI: earlier generation version of TROPOMI with coarser resolution, but longer record

Urban and Point Sources Resolved with TROPOMI

Annual multiyear mean TROPOMI NO$_2$ [10^{15} molecules cm^{-2}]
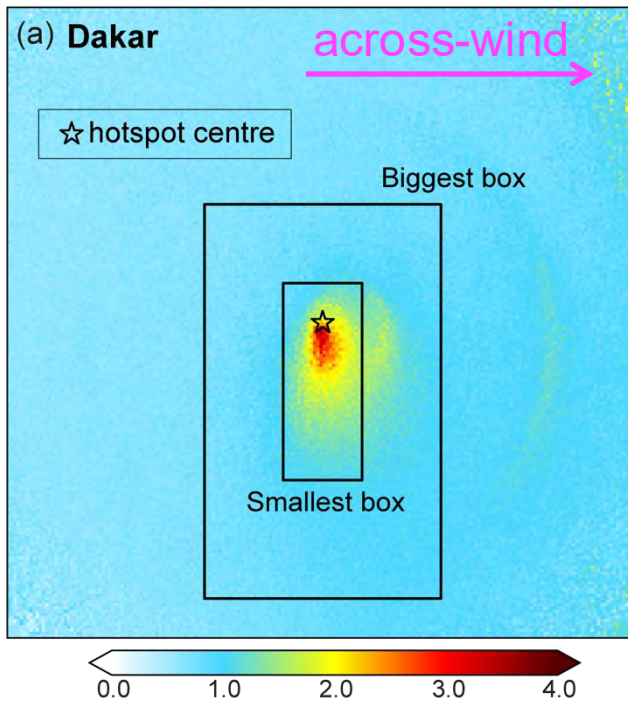
Oversample 4 years of TROPOMI data to finer scale (~2 km) than nadir resolution

Identify 32 isolated hotspots: most urban, 4 power plants
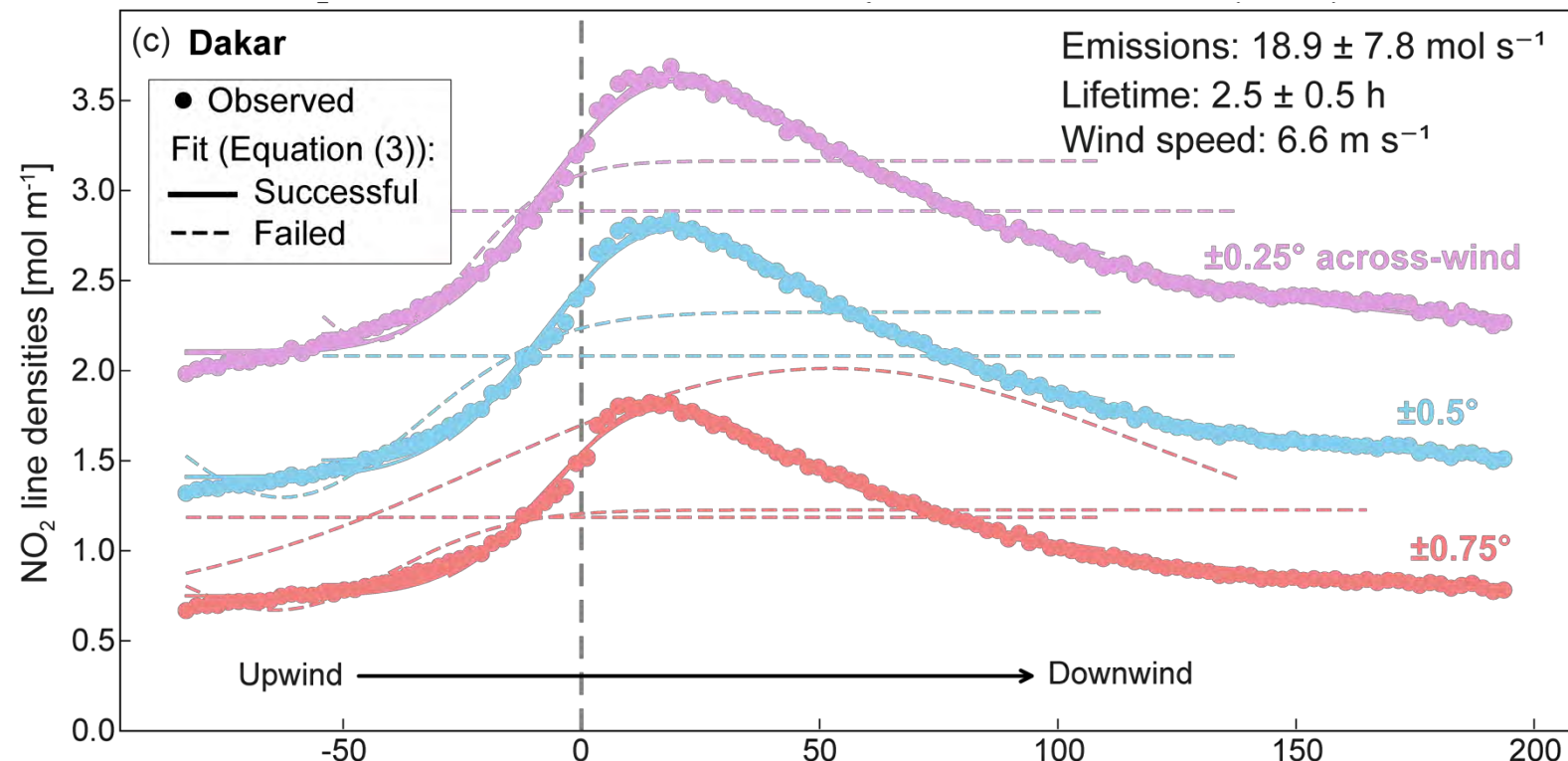
Boxes: dashed if attempt to calculate emissions fails; solid if succeeds

Hotspot NO$_x$ Emissions Inversion Method

Wind rotate TROPOMI NO$_2$ about the hotspot centre

Sum across-wind NO$_2$ to yield 1D line densities and apply an Exponentially Modified Gaussian (EMG) fit
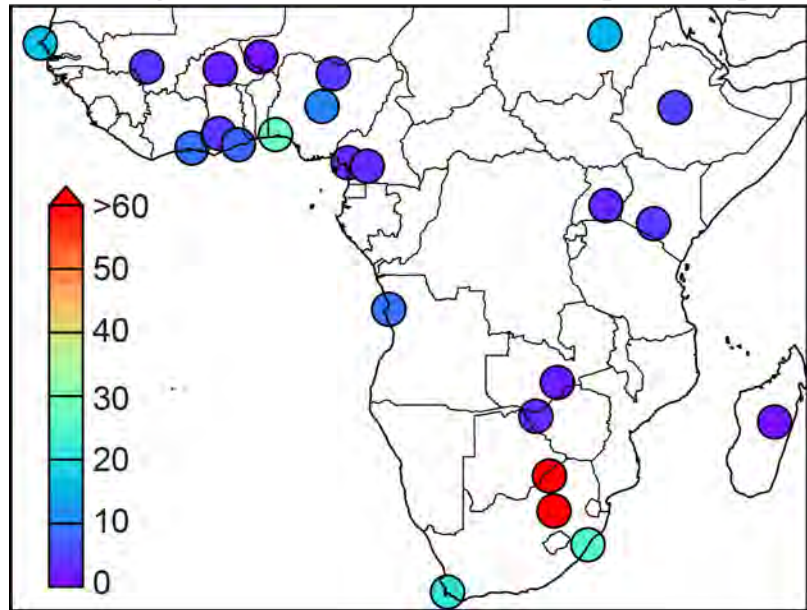
29 out of 36 successful fits for Dakar (Senegal) yielding the following quantities:
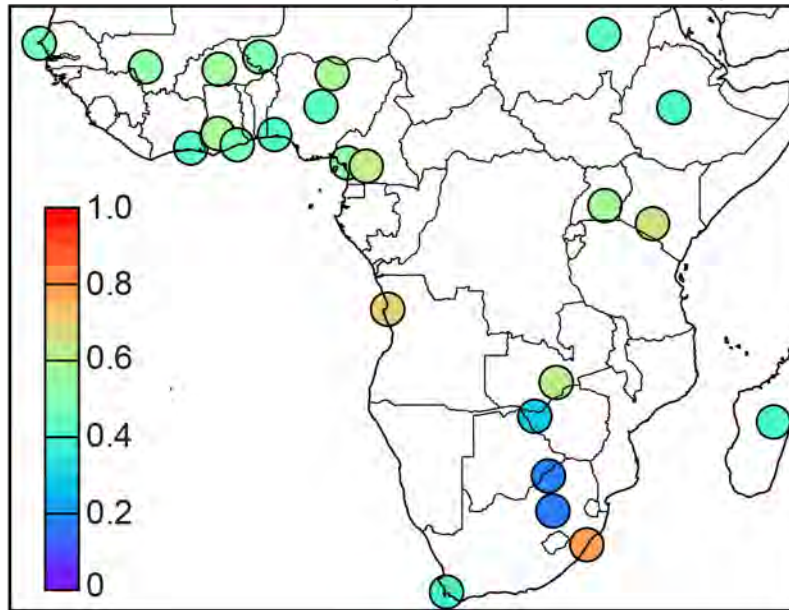
18.9±7.8 mol NO$_x$ emitted s^{-1}, 2.5±0.5 h effective lifetime, 6.6 m s^{-1} wind speed

# NO$_x$ Emissions for All Successful Hotspots
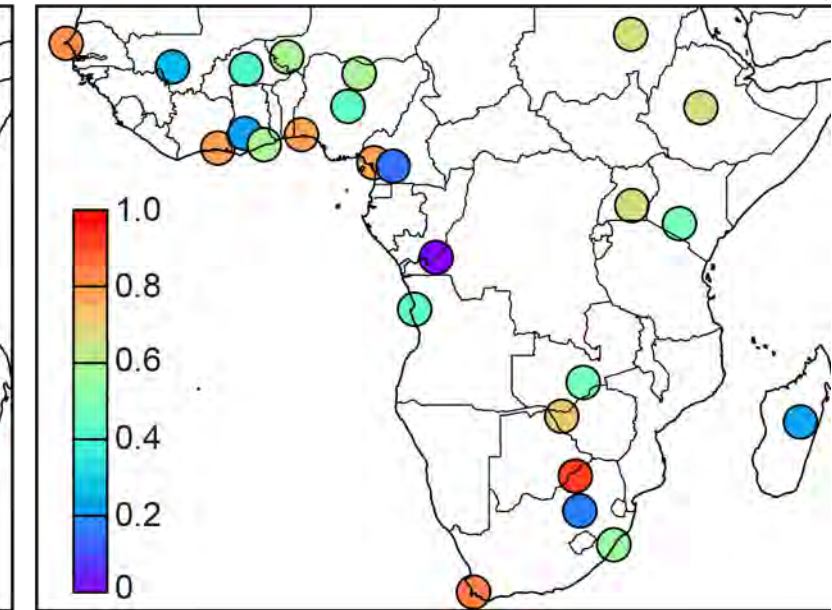
(a) Top-down NO$_x$ emissions [mol s^{-1}]

(b) Relative error (error / emissions)

(c) Relative success (successful / total fits)

Derived emissions for 24 hotspots compared to at most 5 Sub-Saharan hotspots in past studies

Emissions total 207.3 kilotonnes NO

Most hotspots very small (<10 mol s^{-1}) sources of NO$_x$ compared to urban hotspots in Southeast and Southeast Asia (> 60 mol s^{-1} for Delhi and Dhaka [Lu et al., 2025])

Are Power Plant Hotspot NO$_x$ Emissions Accurate?

South Africa power plant emissions measured with Continuous Emissions Monitoring Systems (CEMS)
(https://www.eskom.co.za/dataportal/emissions/ael/)

Matimba and Medupi:

CEMS: 74.1 mol s^{-1}

Top-down (this work): 69.8 ± 25.7 mol s^{-1}
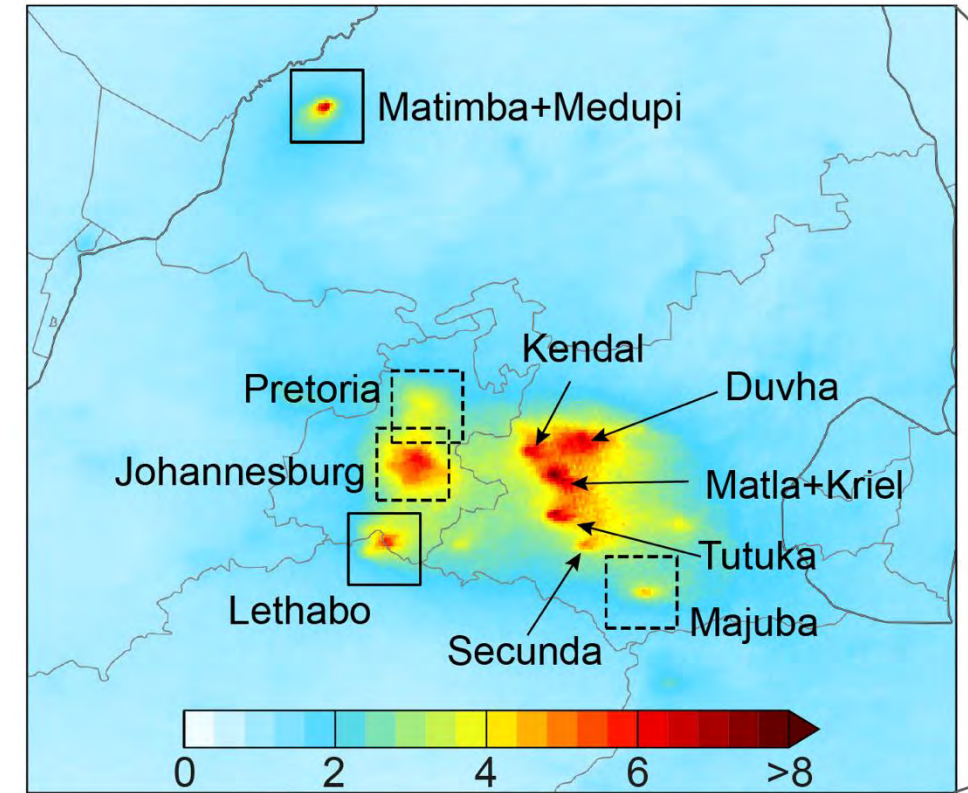
Top-down (Beirle et al., 2023): 82.3 ± 18.7 mol s^{-1}

Lethabo:

CEMS: 65.2 mol s^{-1}

Top-down (this work): 70.4 ± 23.8 mol s^{-1}
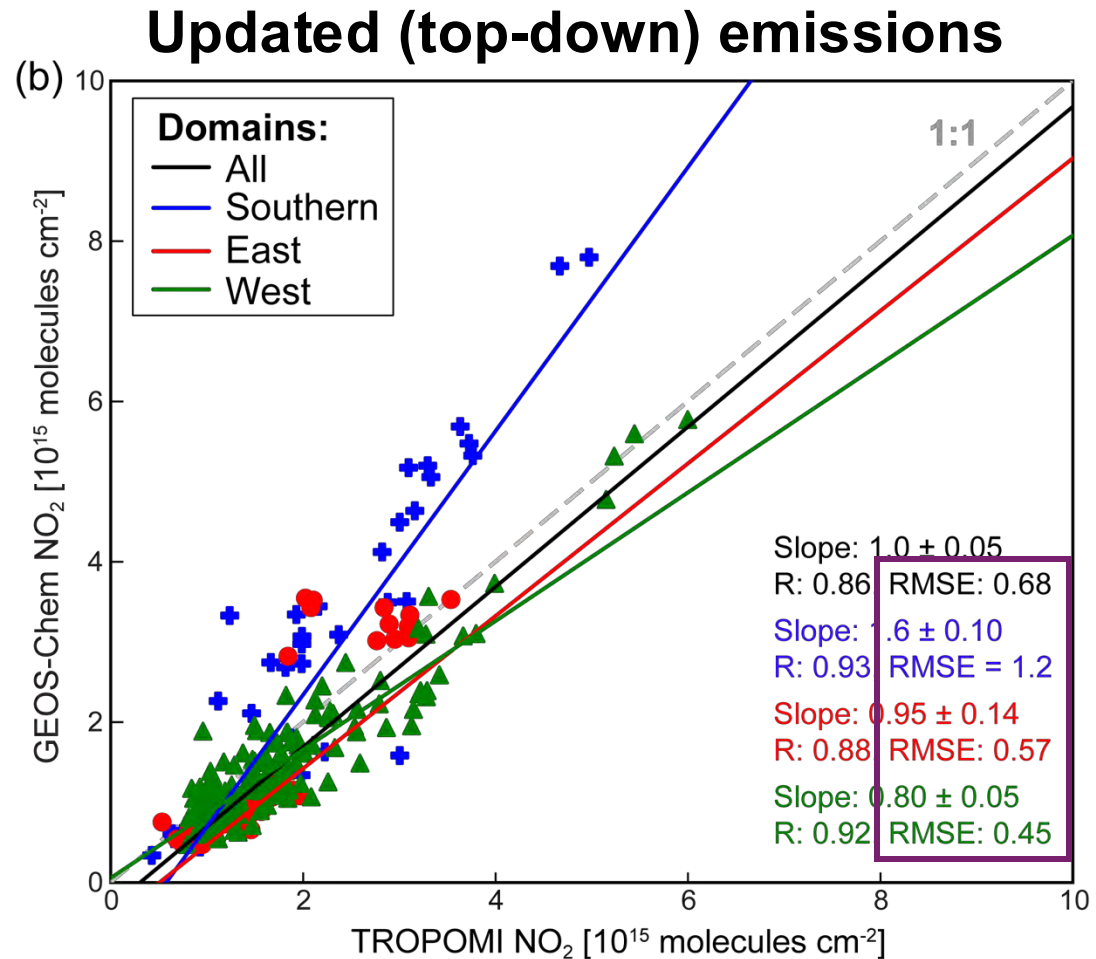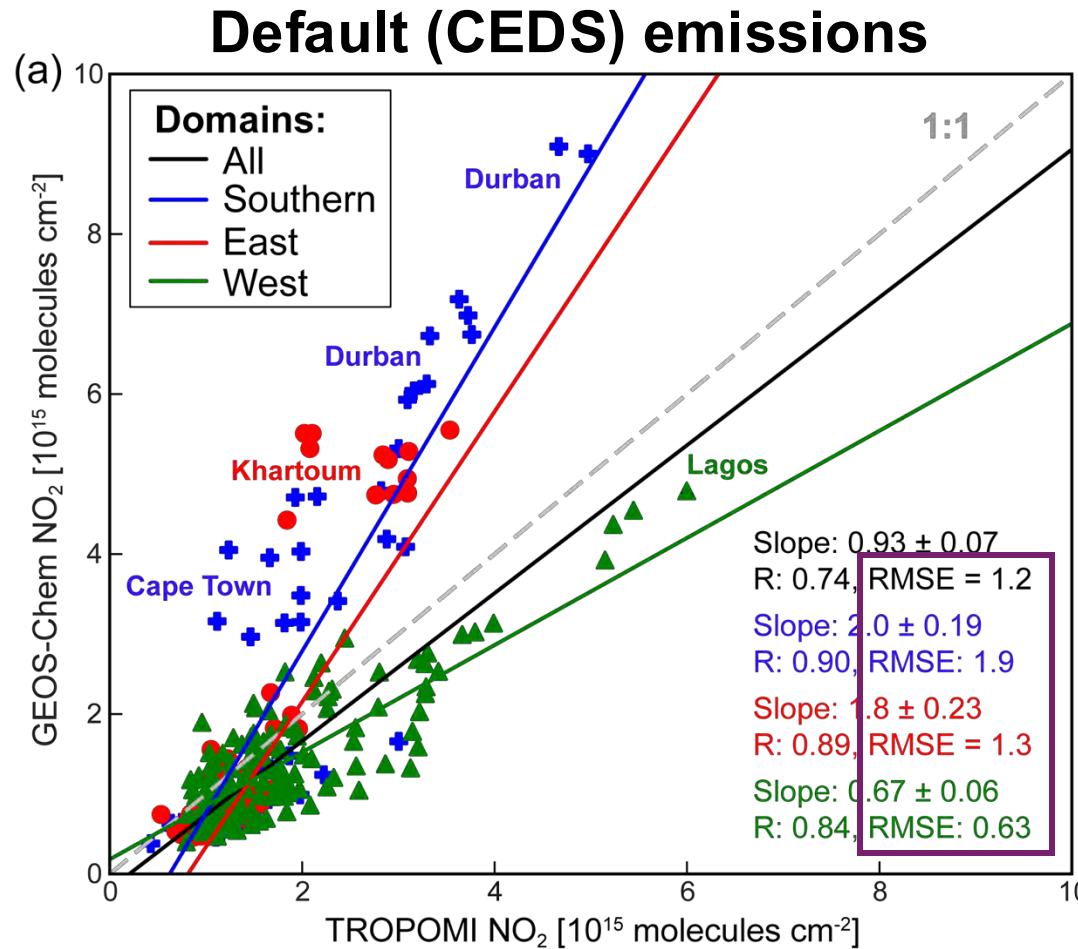
Top-down (Beirle et al., 2023): 67.7 ± 14.7 mol s^{-1}

Our values are within 18-20% of CEMS and within 4-15% of an alternate top-down approach
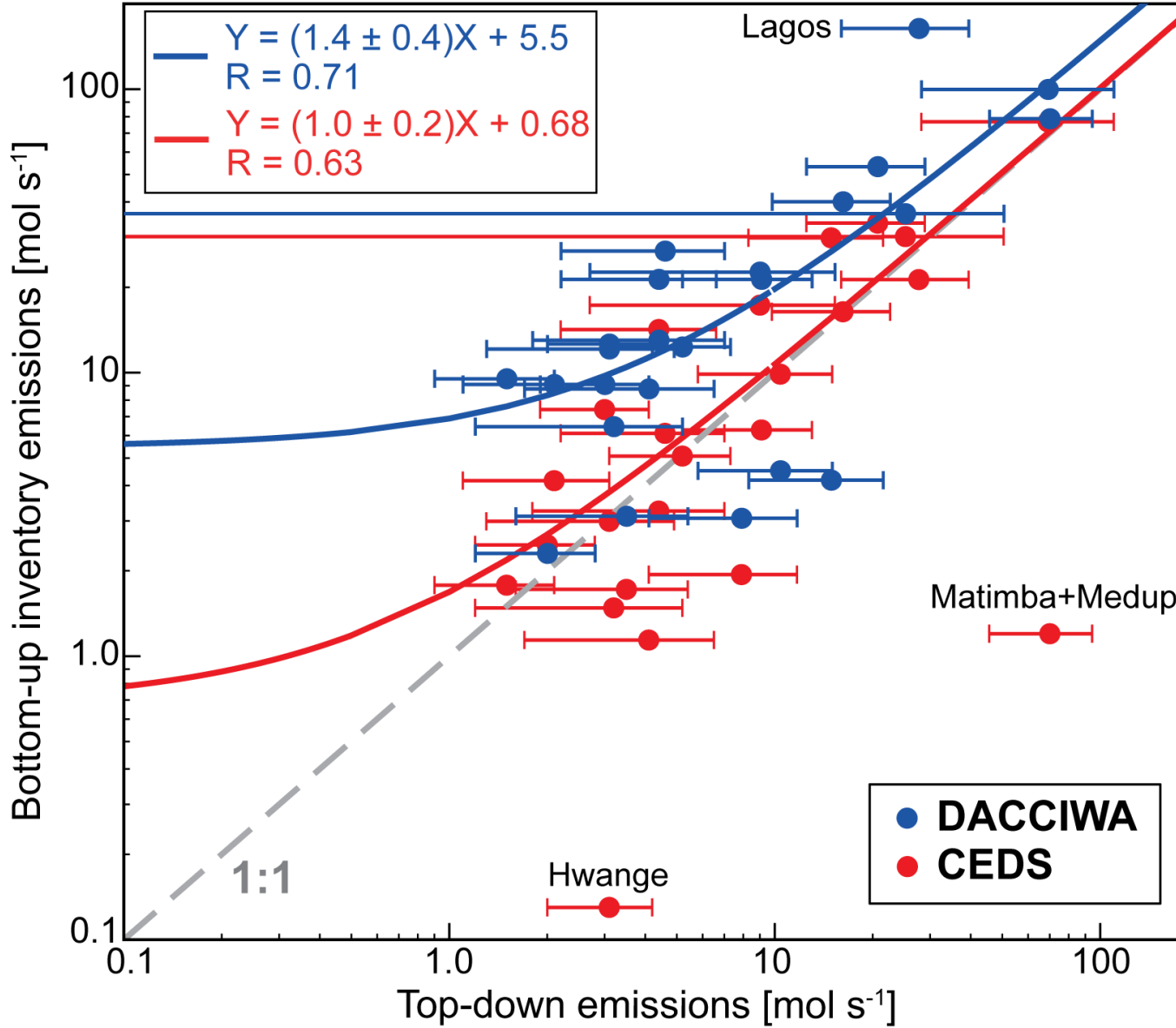
# Are Urban Hotspot NOₓ Emissions Accurate?

Emissions → **GE🌐S-Chem** → **NO₂ column densities**

Default (CEDS) emissions

Updated (top-down) emissions

Urban CEDS emissions total 159 kilotonnes NO, whereas top-down total 135 kilotonnes NO

Top-down versus inventory Hotspot NO$_x$ Emissions

Comparison on log-log scale

DACCIWA: regional emissions inventory for Africa

CEDS: global emissions inventory widely used in models

<u>CEDS</u> on average consistent (slope = 1.0), but missing Medupi and Matimba power plants and underestimate Hwange power plant

<u>DACCIWA</u> on average 40% more than top-down emissions. Almost factor of 6 more for Lagos!

Second Part Summary

Derived annual NO_x emissions for 24 isolated hotspots (21 urban, 3 power plants)

Annual hotspot emissions total 207.3 kilotonnes NO

Urban hotspot emissions range from < 2 mol s^{-1} for Antananarivo in Madagascar to 27.7 ± 11.7 mol s^{-1} for the megacity Lagos in Nigeria

Coal-fired power plant emissions are 2.7 ± 0.9 mol s^{-1} for Hwange in Zimbabwe and similar (~70 mol s^{-1}) for Lethabo and combined plumes of Medupi and Matimba in South Africa

Top-down estimates are within ±20% of measured CEMS

CEDS inventory urban hotspot emissions decline from 159 to 135 kt NO and model root mean squared error declines from 1.2×10^{15} to 0.71×10^{15} molecules cm^{-2}